

**Combined Analysis: texture, structure, microstructure, phase, stress, reflectivity
(multiphase bulks and thin films, x-rays and neutron diffraction): some case studies**

Daniel Chateigner
CRISMAT-ENSICAEN (Caen-France)

**Bi2223
Superconductors**

**PCT & PMN-PT
Ferroelectrics**

**Irradiated
FAP ceramics**



**$\text{Ca}_3\text{Co}_4\text{O}_9$
Thermoelectrics**

**nano-Si
thin films**

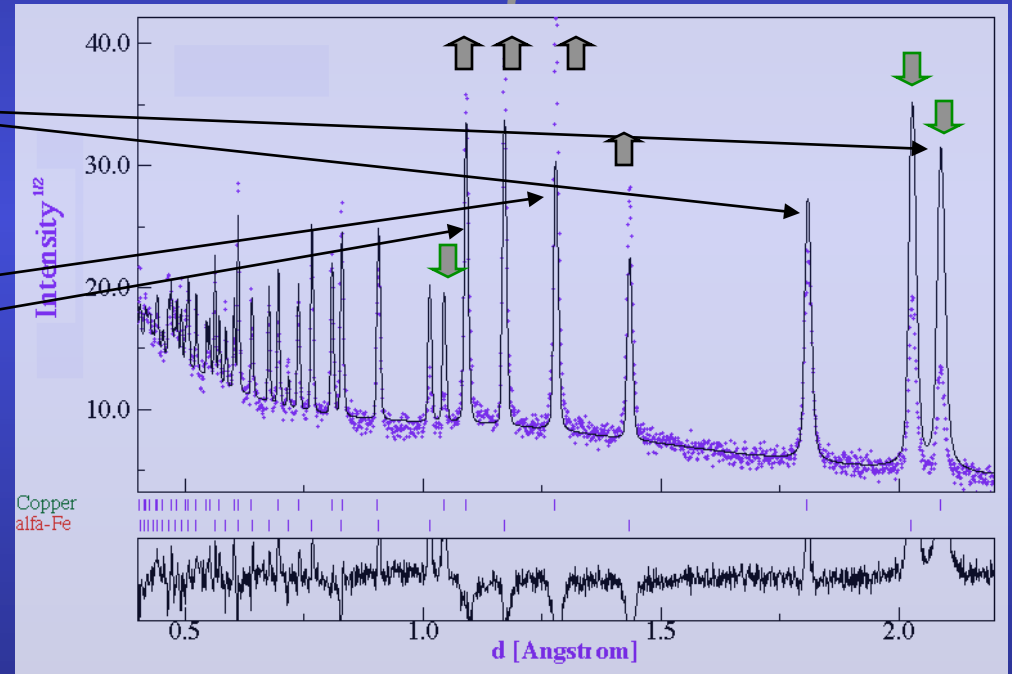
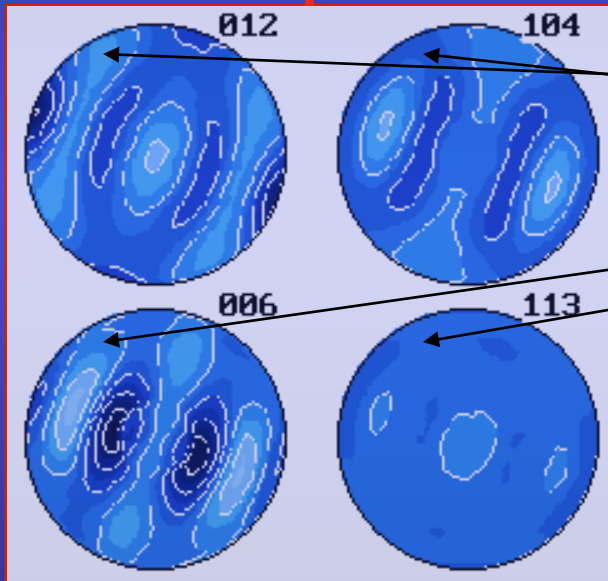


Texture from Spectra

Orientation Distribution Function (ODF)

From pole figures

From spectra



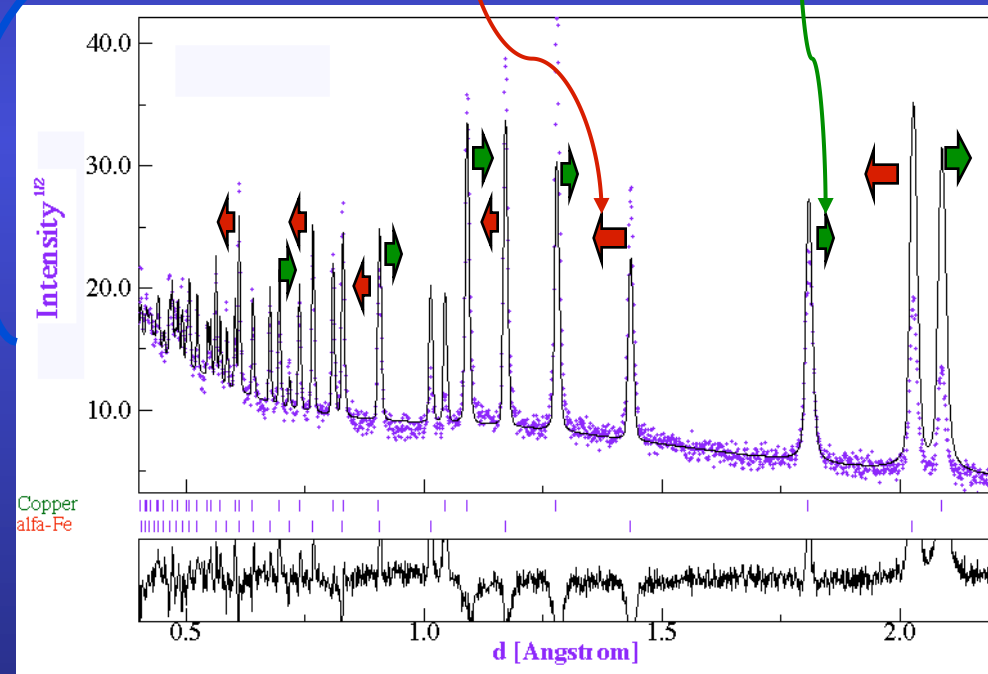
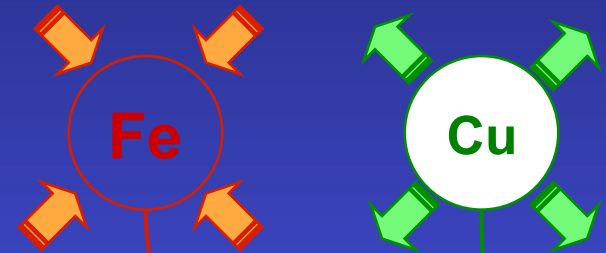
Residual Stresses and Rietveld

- Macro elastic strain tensor (I kind)
- Crystal anisotropic strains (II kind)

C

Macro and micro stresses

Applied macro stresses



Textured samples: Reuss, Voigt, Hill, Bulk geometric mean approaches

How it works (Combined)

$$I_i^{calc}(\chi, \phi) = \sum_{n=1}^{Nphases} S_n \sum_k L_k |F_{k;n}|^2 S(2\theta_i - 2\theta_{k;n}) P_{k;n}(\chi, \phi) A + bkg_i$$

Texture

$$P_k(\chi, \phi) = \int_{\varphi} f(g, \varphi) d\varphi$$

- from Generalized Spherical Harmonics:

$$P_k(\chi, \phi) = \sum_{l=0}^{\infty} \frac{1}{2l+1} \sum_{n=-l}^l k_l^n(\chi, \phi) \sum_{m=-l}^l C_l^{mn} k_n^{*m}(\Theta_k \phi_k)$$

$$f(g) = \sum_{l=0}^{\infty} \sum_{m,n=-l}^l C_l^{mn} T_l^{mn}(g)$$

- from the WIMV (left) iterative process or entropy maximisation (right):

$$f^{n+1}(g) = N_n \frac{f^n(g) f^0(g)}{\left(\prod_{h=1}^1 \prod_{m=1}^{M_h} P_h^n(\mathbf{y}) \right)^{\frac{1}{M_h}}}$$

$$f^{n+1}(g) = f^n(g) \prod_{m=1}^{M_h} \left(\frac{P_h(\mathbf{y})}{P_h^n(\mathbf{y})} \right)^{\frac{r_n}{M_h}}$$

Layering

$$C_{\chi}^{\text{top film}} = g_1 (1 - \exp(-\mu T g_2 / \cos \chi)) / (1 - \exp(-2\mu T / \sin \omega \cos \chi))$$

$$C_{\chi}^{\text{cov. layer}} = C_{\chi}^{\text{top film}} \left(\exp(-g_2 \sum \mu'_i T'_i / \cos \chi) \right) / \left(\exp(-2 \sum \mu'_i T'_i / \sin \omega \cos \chi) \right)$$

Popa anisotropic shapes & microstrains

$$\begin{aligned} \langle R_h \rangle &= R_0 + R_1 P_2^0(x) + R_2 P_2^1(x) \cos \varphi + R_3 P_2^1(x) \sin \varphi + R_4 P_2^2(x) \cos 2\varphi + R_5 P_2^2(x) \sin 2\varphi + \\ \langle \varepsilon_h^2 \rangle E_h^4 &= E_1 h^4 + E_2 k^4 + E_3 \ell^4 + 2E_4 h^2 k^2 + 2E_5 \ell^2 k^2 + 2E_6 h^2 \ell^2 + 4E_7 h^3 k + 4E_8 h^3 \ell + 4E_9 k^3 h + \\ &4E_{10} k^3 \ell + 4E_{11} \ell^3 h + 4E_{12} \ell^3 k + 4E_{13} h^2 k \ell + 4E_{14} k^2 h \ell + 4E_{15} \ell^2 k h \end{aligned}$$

Roughness and/or microabsorption

$$R^{\text{rough}}(q_z) = R(q_z) \exp(-q_{z,0} q_{z,1} \sigma^2) \quad \text{Low-angles (reflectivity)}$$

$$S_R = 1 - p \exp(-q) + p \exp\left(\frac{-q}{\sin \theta}\right) \quad \text{high-angle (Suortti)}$$

Specular reflectivity: $\mathbf{q}=(0,0,z)$

- Fresnel:

$$R(\mathbf{q}) = \left| \frac{q_z - \sqrt{q_z^2 - q_c^2 + \frac{32i\pi^2\beta}{\lambda^2}}}{q_z + \sqrt{q_z^2 - q_c^2 + \frac{32i\pi^2\beta}{\lambda^2}}} \right|^2 \delta q_x \delta q_y$$

- matrix:

$$R^{flat} = \frac{r_{0,1}^2 + r_{1,2}^2 + 2r_{0,1}r_{1,2} \cos 2k_{z,1}h}{1 + r_{0,1}^2 r_{1,2}^2 + 2r_{0,1}r_{1,2} \cos 2k_{z,1}h}$$

- Born approximation:

$$R(q_z) = r \cdot r^* = R_F(q_z) \left| \frac{1}{\rho_s} \int_{-\infty}^{+\infty} \frac{d\rho(z)}{dz} e^{iq_z z} dz \right|^2$$

Phase

$$W_{\Phi} = \frac{S_{\Phi} Z_{\Phi} M_{\Phi} V_{\Phi}}{\sum_{i=1}^{N_{\Phi}} S_i Z_i M_i V_i}$$

Strain-Stress

$$\boldsymbol{\varepsilon}(\mathbf{X}) = \boldsymbol{\varepsilon}^I + \boldsymbol{\varepsilon}^{II}(\mathbf{X}) + \boldsymbol{\varepsilon}^{III}(\mathbf{X})$$

$$\begin{aligned} \langle \boldsymbol{\varepsilon}_h(\mathbf{y}) \rangle_{V_d} &= \frac{1}{V_d} \int_{V_d} (\boldsymbol{\varepsilon}_{33}^I + \boldsymbol{\varepsilon}_{33}^{II} + \boldsymbol{\varepsilon}_{33}^{III}) dV \\ &= (\boldsymbol{\varepsilon}_{11}^I \cos^2 \phi + \boldsymbol{\varepsilon}_{12}^I \sin 2\phi + \boldsymbol{\varepsilon}_{22}^I \sin^2 \phi - \boldsymbol{\varepsilon}_{33}^I) \sin^2 \psi + \boldsymbol{\varepsilon}_{33}^I + \\ &\quad (\boldsymbol{\varepsilon}_{13}^I \cos \phi + \boldsymbol{\varepsilon}_{23}^I \sin \phi) \sin 2\psi + \frac{1}{V_d} \int_{V_d} (\boldsymbol{\varepsilon}_{33}^{IIe} + \boldsymbol{\varepsilon}_{33}^{IIa} + \boldsymbol{\varepsilon}_{33}^{IIpi}) dV \\ &= \frac{\langle d(hkl, \phi, \psi) \rangle_{V_d} - d_0(hkl)}{d_0(hkl)} \end{aligned}$$

Isotropic samples:

Tri-, bi-, uni-axial stress states

Textured samples:

Tri-, bi-, uni- stress states
+ ODF + SDF + model

$$\begin{aligned} \langle E(\mathbf{g}) \rangle_{V_d} &= \frac{1}{V_d} \int_{V_d} E^{SC}(\mathbf{g}) f(\mathbf{g}) d\mathbf{g} \quad \Rightarrow \quad C_{ijkl}^M \neq \left(S_{ijkl}^M \right)^{-1} \\ &= \left(\prod_{V_d} E^{SC}(\mathbf{g}) f(\mathbf{g}) d\mathbf{g} \right)^{\frac{1}{V_d}} \quad \Rightarrow \quad C_{ijkl}^M = \left(S_{ijkl}^M \right)^{-1} \end{aligned}$$

Reuss, Voigt, Hill

Geometric mean, VPSC

Minimum experimental requirements

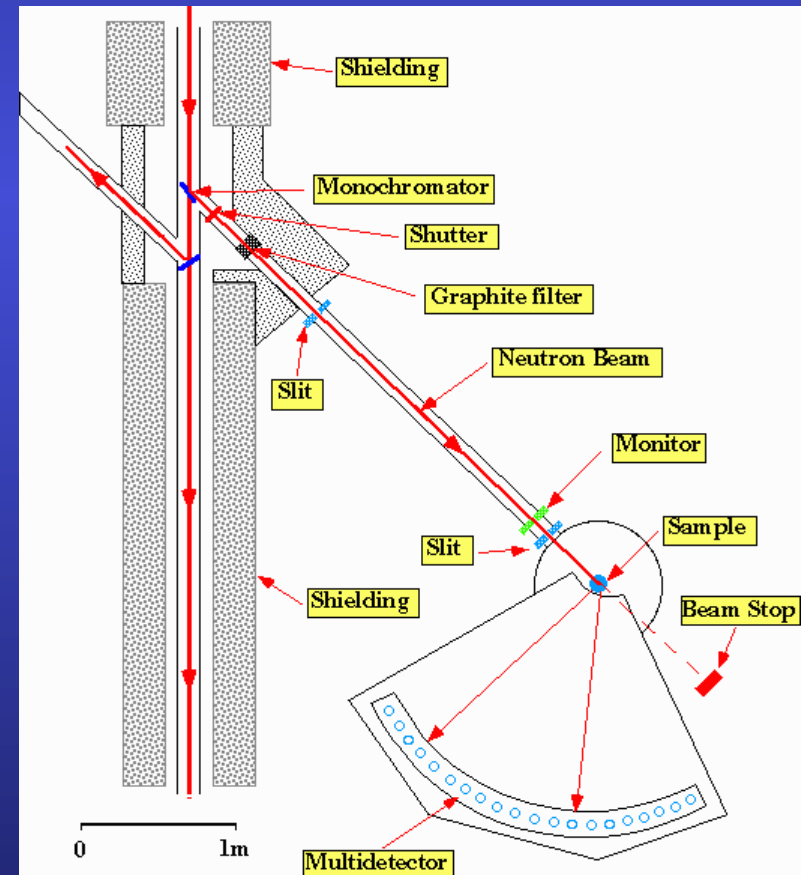
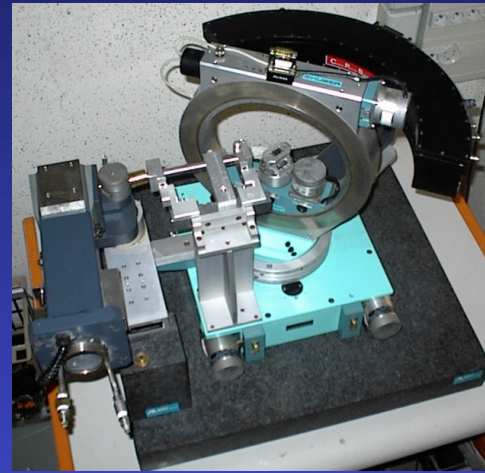
1D or 2D Detector + 4-circle diffractometer
(X-rays and neutrons)
CRISMAT, ILL

+

~1000 experiments (2θ diagrams)
in as many sample orientations

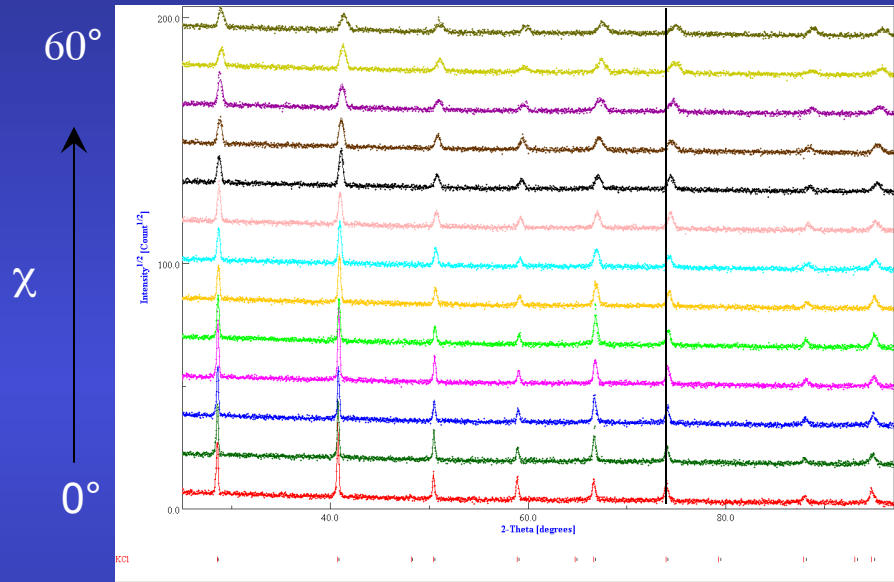
+

Instrument calibration
(peaks widths and shapes,
misalignments, defocusing ...)

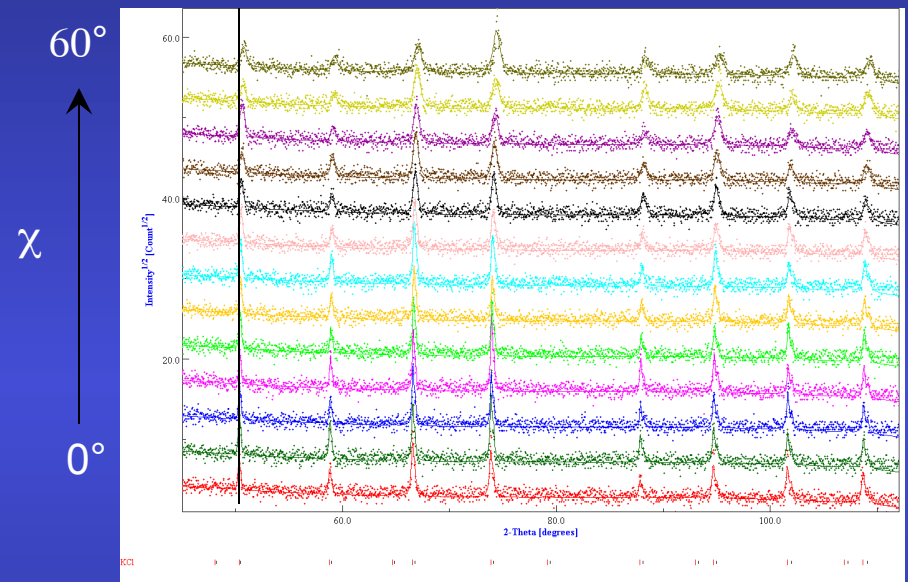


Calibration

$\omega = 20^\circ$



$\omega = 40^\circ$



KCl, LaB₆ ...



FWHM (ω , χ , 2θ ...)
2 θ shift
gaussianity
asymmetry
misalignments ...

Methodology implementation

L. Lutterotti, Trento

User friendly interface

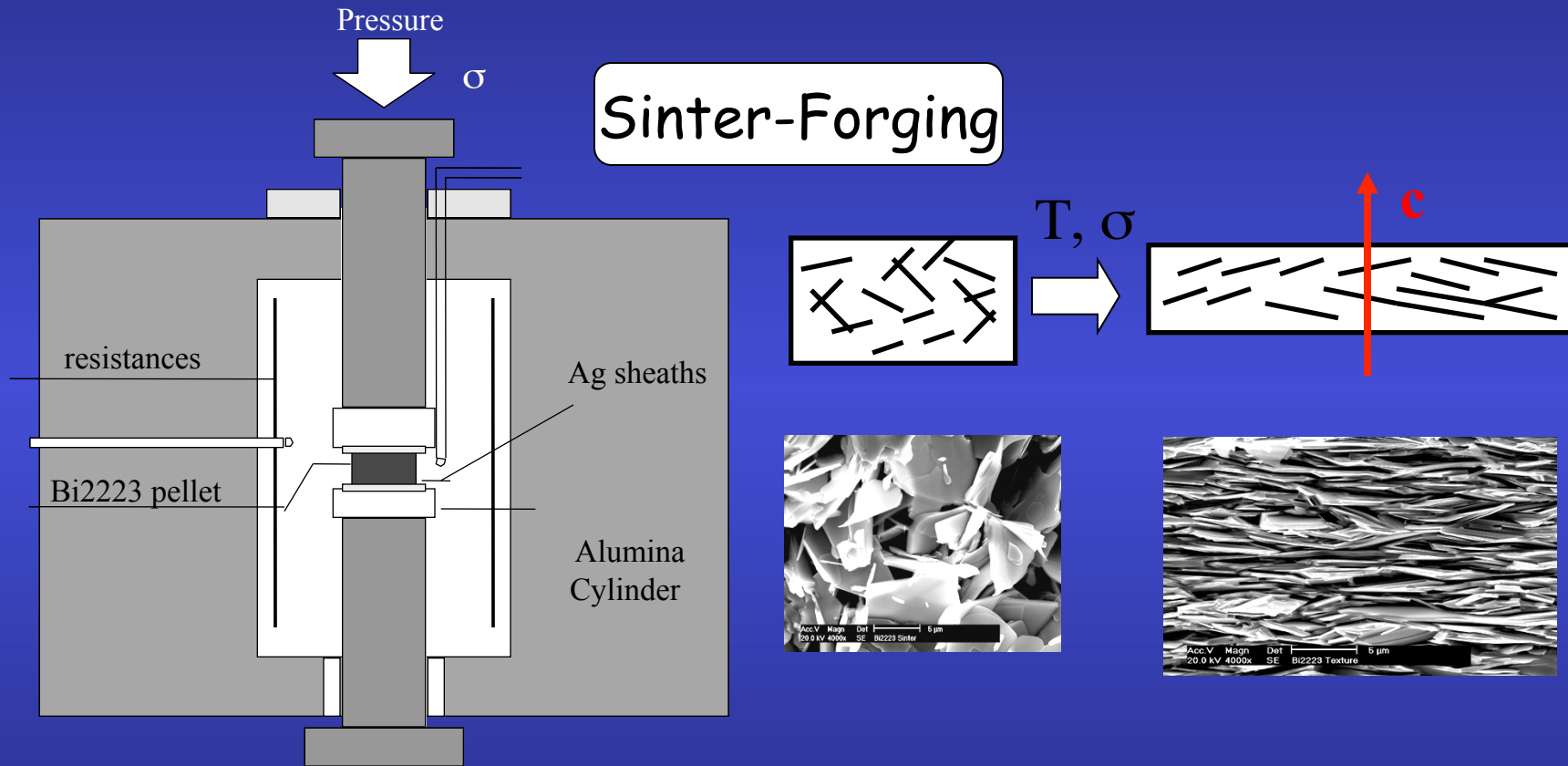
The screenshot shows the MAUD software interface. At the top, there's a 'TreeTable' window with columns for Name, Value, Error, and Status. It lists parameters like atom sites and cell length, with statuses such as 'Fixed', 'Refined', and 'Equal to'. Below this is the 'Refinement wizard' with several radio button options for refining different sets of parameters (Background and scale, Previous + basic phase, Previous + microstructure, Previous + crystal structure, All parameters for texture). A 'Pole Figure plot' is visible on the left, and a 3D model of a crystal structure is shown at the bottom left.

This screenshot shows the MAUD software interface with the 'Microstructure' dialog box open. The dialog has several sections: 'Line Broadening' with a dropdown menu set to 'Delf' and other options like 'Popa LB', 'Trento', and 'Distributions'; 'Size-Strain model' set to 'Popa'; 'Antiphase boundary model' set to 'none abm'; and 'Planar defects model' set to 'none pd'. There are also 'Options' buttons for each section. Below the dialog, there's a 3D model of a yellow crystal and two XRD patterns. The bottom pattern shows a full scan from 50.0 to 150.0 degrees 2-Theta, while the top pattern is a zoomed-in view from 130.0 to 140.0 degrees 2-Theta. The status bar at the bottom right indicates 'ation computation or sample: CPD-Y203' and 'ures: 14267.7133202'.

Java codes
Java web start updates

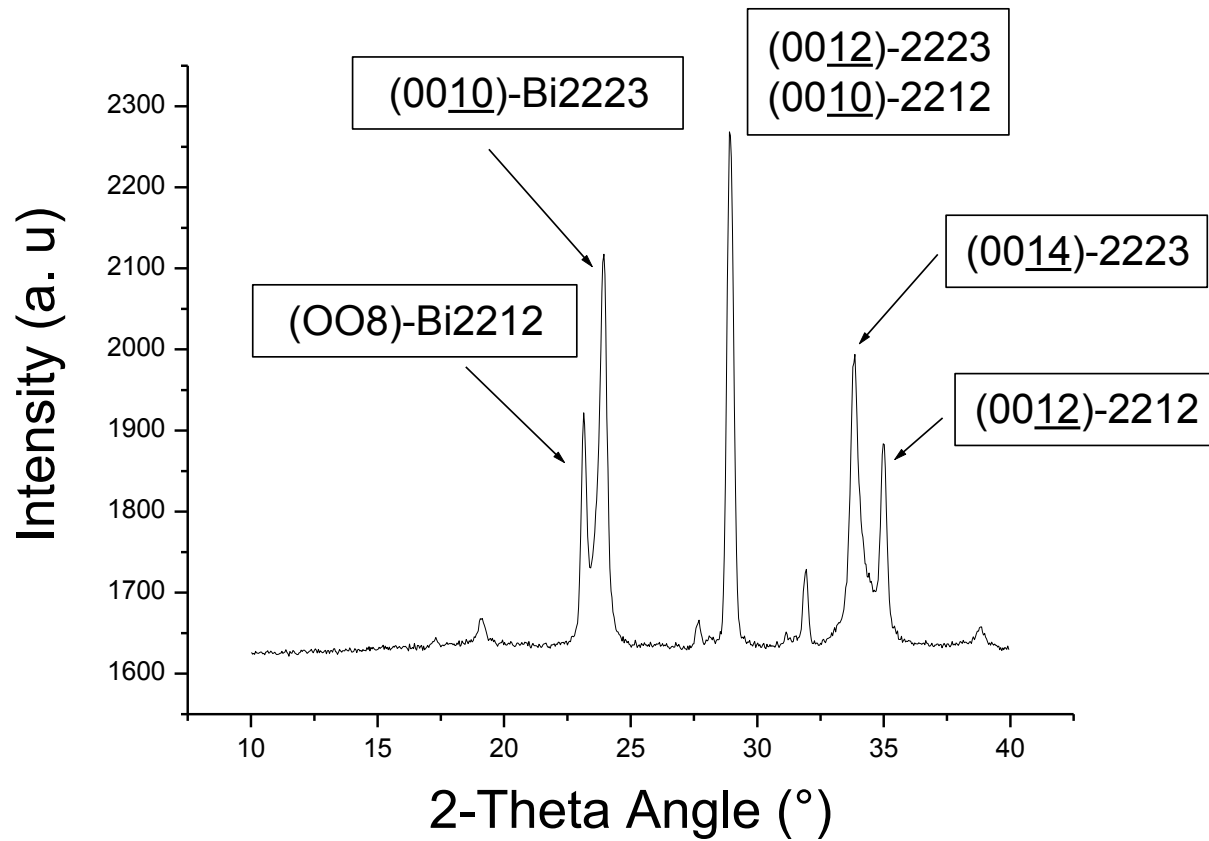
Bi2223 compounds

E. Guilmeau, CRISMAT

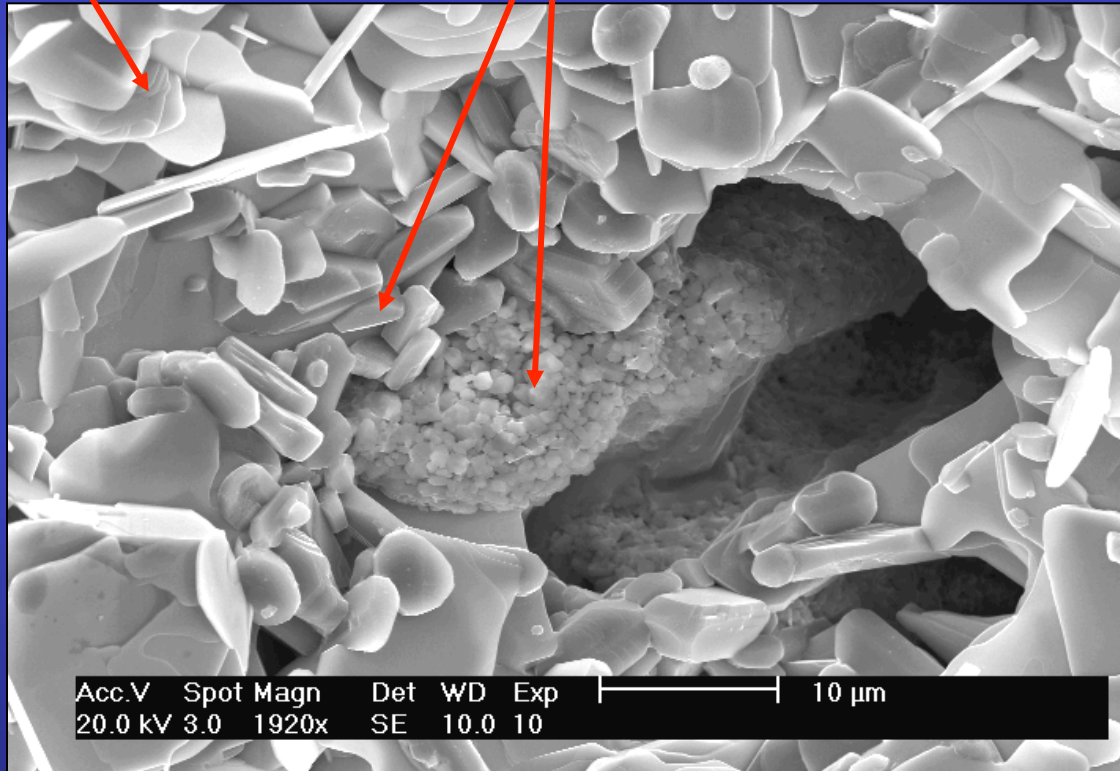


Grain alignment \Rightarrow \nearrow J_c

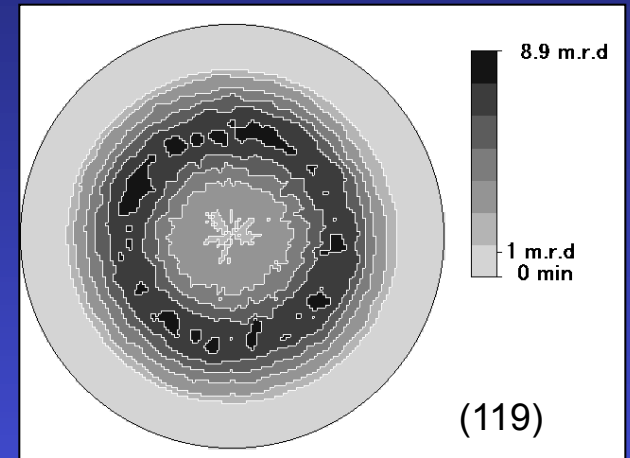
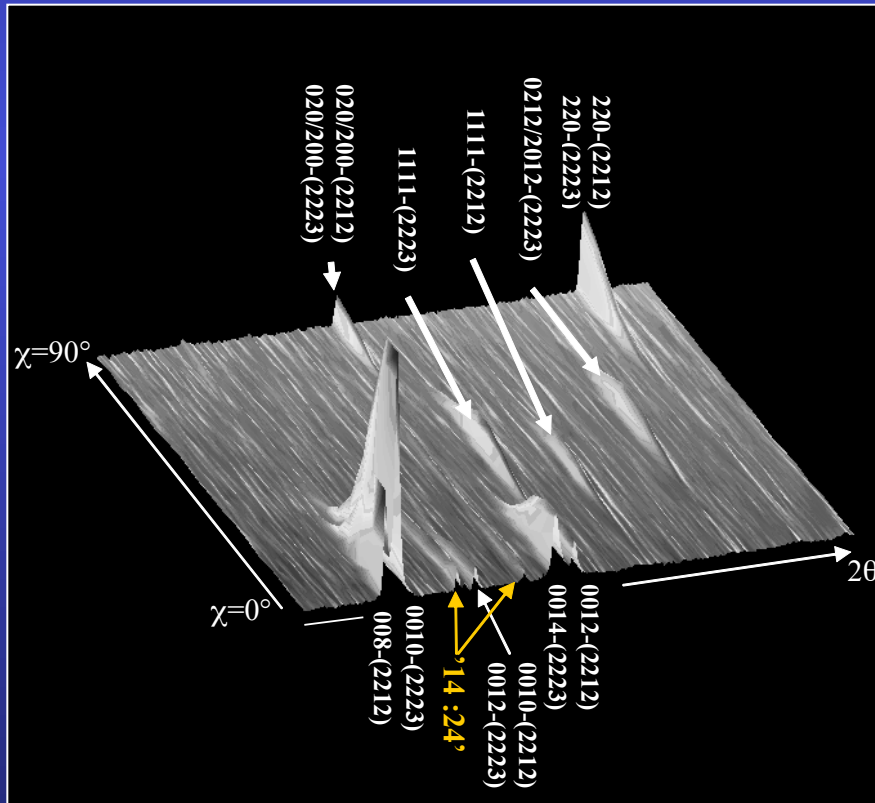
(00 l) Texture



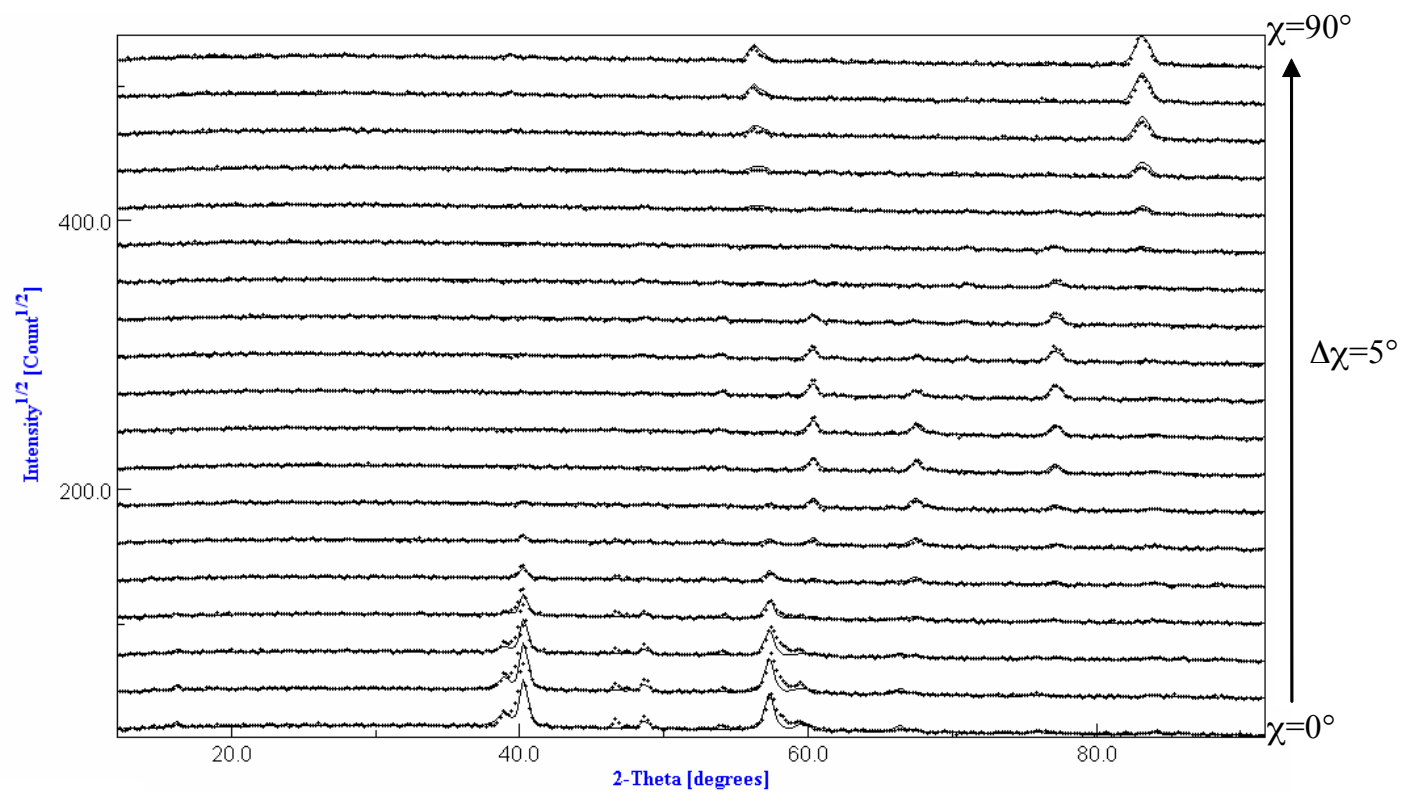
Bi2212 + Secondary phases \longrightarrow Bi2223



Combined Analysis



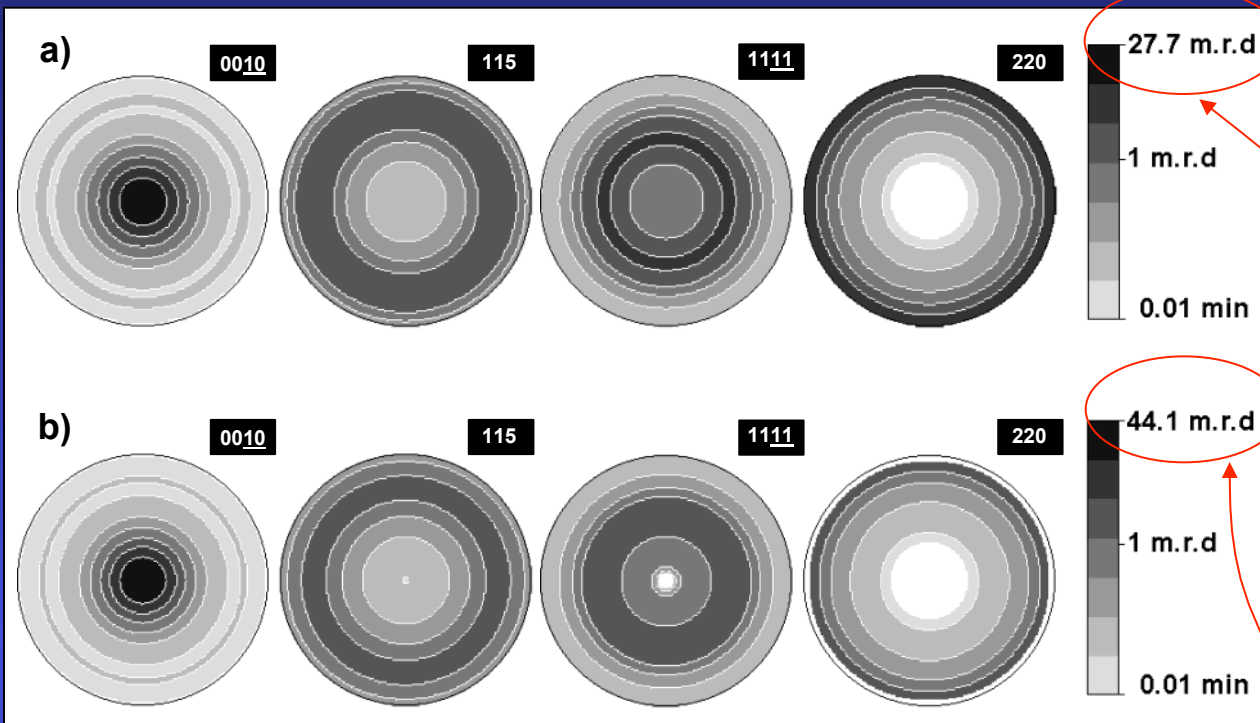
- Neutrons
- Sample: $\sim 70 \text{ mm}^3$
- 2θ patterns for $\chi=0^\circ$ to 90°
- No φ rotation (fibre texture).



2223
2212



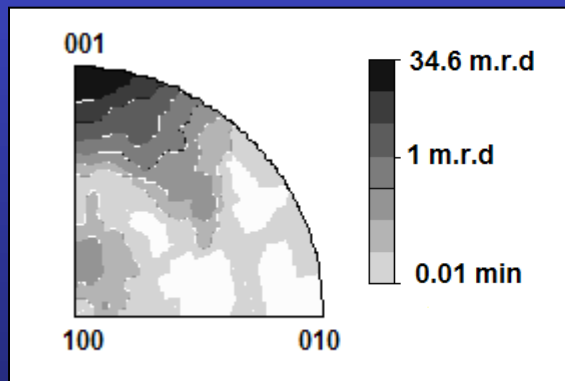
$R_w=9.12$
 $RP=16.24$



Logarithmic density scale, equal area projection

*Recalculated
(WIMV)*

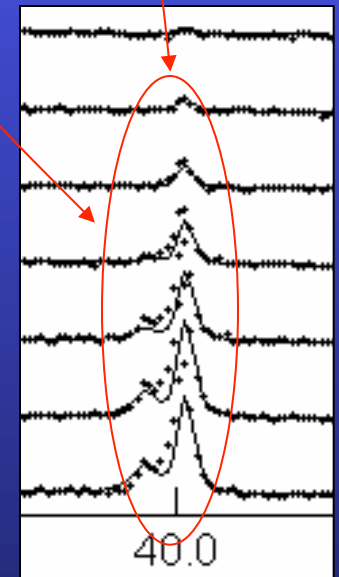
*Extracted
(Le Bail)*



Logarithmic density scale, equal area projection

Stacking faults and/or intergrowth on the c-axis
 → New periodicities and peaks characterized with intermediate c parameters.

However, no algorithm is included to solve intergrowths in the combined approach.



40.0

Effect of the sinter-forging treatment on the texture development, crystal growth, transport properties

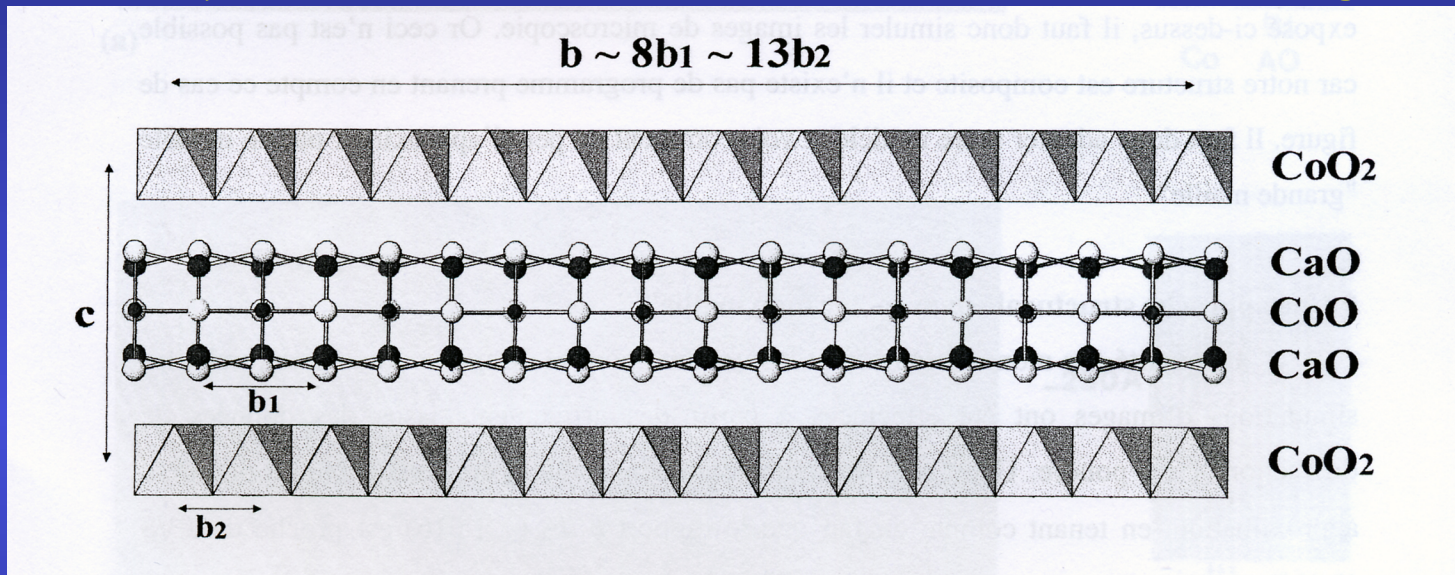
Sinter-forging dwell time (h)	Orientation Distribution Max (m.r.d.)		% Bi2223	Cell parameters (Å)		Crystallite size Bi2223 (nm)	Rb (%)	Rw (%)	Rexp (%)	RP0 (%)	RP1 (%)	J_c (A/cm ²)
	Bi2212	Bi2223		Bi2223	Bi2212							
20	21.8	20.7	59.9±1.3	a=5.419(3) b=5.391(3) c=37.168(3)	a=5.414(3) b=5.393(3) c=30.800(3)	205±7	7.56	11.1	4.55	17.74	10.56	12500
50	24.1	24.4	72.9±2.9	a=5.419(3) b=5.408(3) c=37.192(3)	a=5.416(3) b=5.396(3) c=30.806(3)	273±10	7.54	11.37	4.58	17.05	11.04	15000
100	31.5	25.2	84.4±4.6	a=5.410(3) b=5.405(3) c=37.144(3)	a=5.412(3) b=5.403(3) c=30.752(3)	303±10	5.4	8.04	3.69	13.54	9.31	19000
150	65.4	27.2	87.0±4.1	a=5.417(3) b=5.403(3) c=37.199(3)	a=5.413(3) b=5.407(3) c=30.792(3)	383±13	6.13	9.12	4.8	16.24	12.25	20000



$Ca_3Co_4O_9$ thermoelectrics

M. Prevel, CRISMAT

$Ca_3Co_4O_9$: Misfit lamellar and modulated Structure, with high thermopower



Two monoclinic sub-systems:

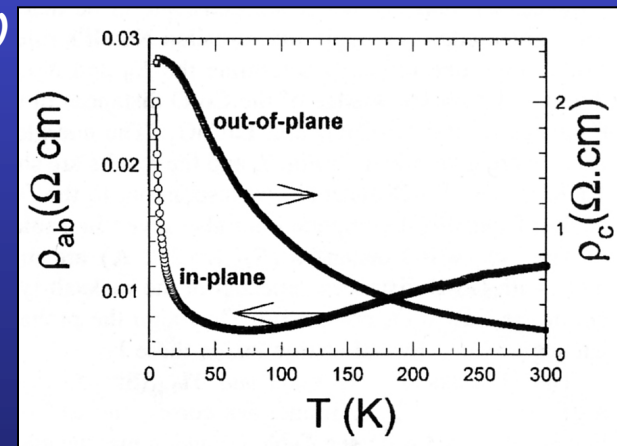
S1 with $a \sim 4.8\text{\AA}$, $b_1 \sim 4.5\text{\AA}$, $c \sim 10.8\text{\AA}$ et $\beta \sim 98^\circ$ (NaCl-type)

S2 with $a \sim 4.8\text{\AA}$, $b_2 \sim 2.8\text{\AA}$, $c \sim 10.8\text{\AA}$ et $\beta \sim 98^\circ$ (CdI_2 -type)

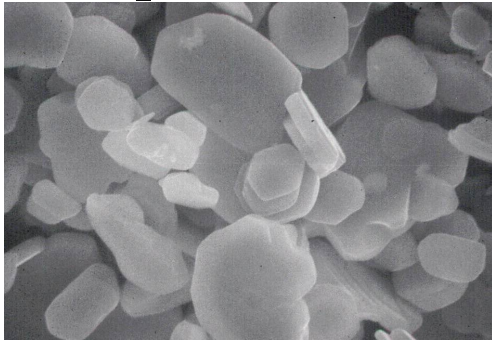
$$\Gamma = \sigma_{ab} / \sigma_c \sim 10$$



Texture

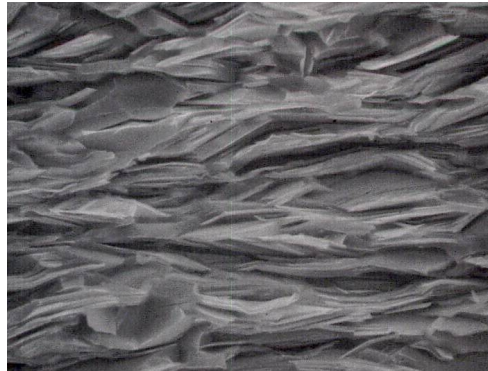


powder



10 μm

Textured bulk

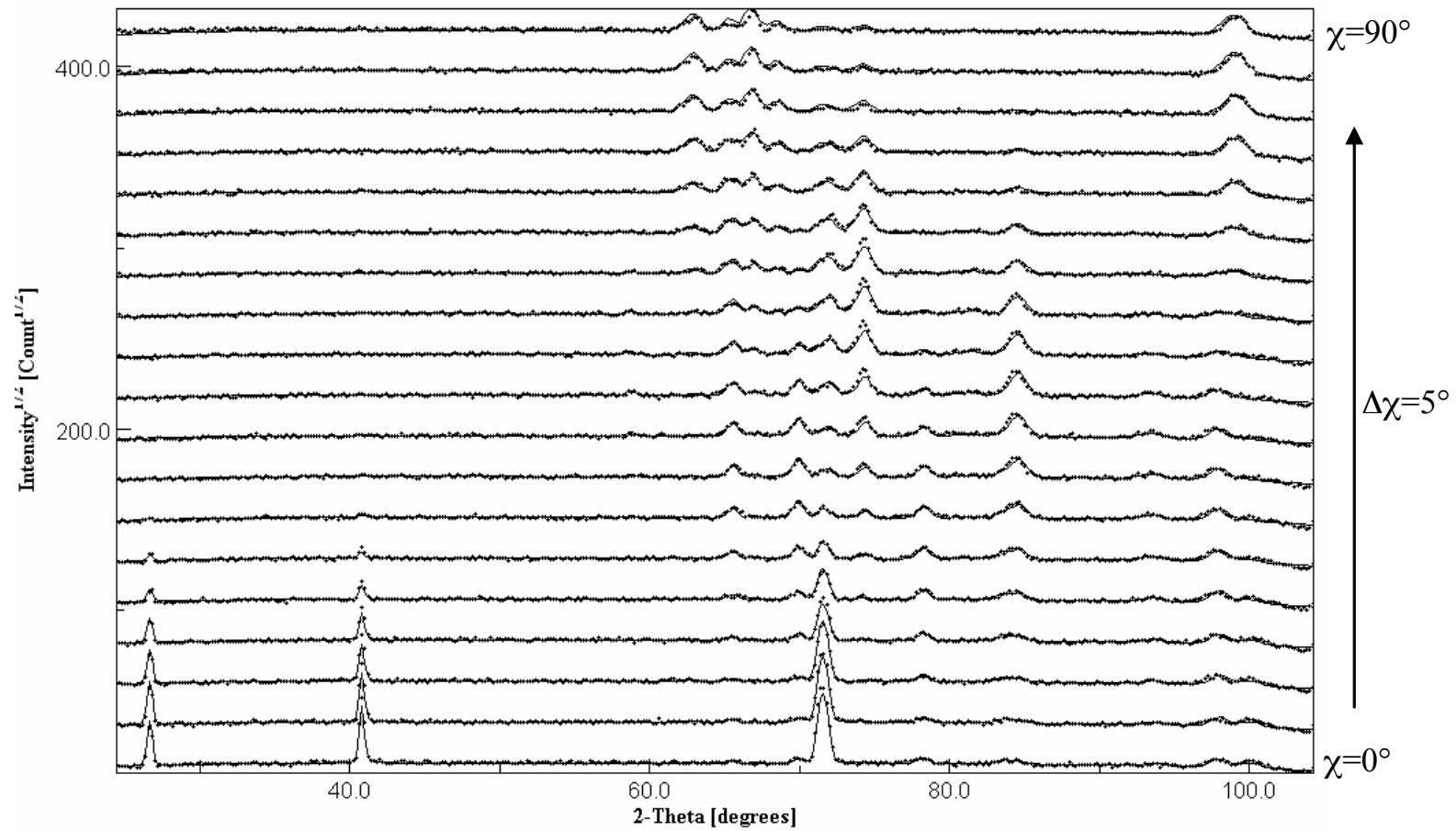


10 μm

*Magnetic alignment
and
Templated Growth
method*

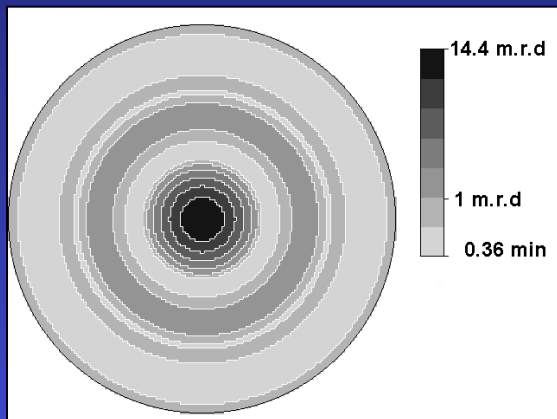
Analysis:

- neutrons
- 3D Supercell: $a=4.8309\text{\AA}$, $b\sim 8b1\sim 13b2\sim 36.4902\text{\AA}$, $c=10.8353\text{\AA}$, $\beta=98.13^\circ$
174 atoms/cell
- Sample : 0.6 cm^3

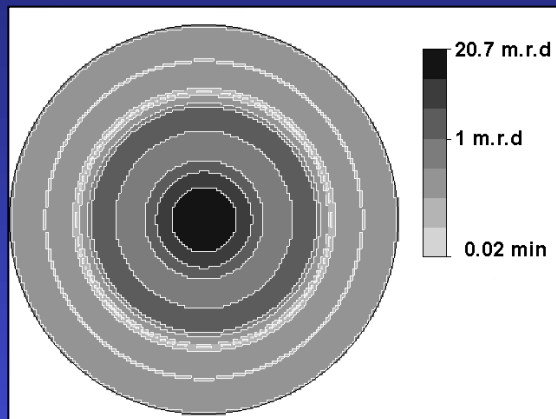


RP=19.7%, Rw=11.9%

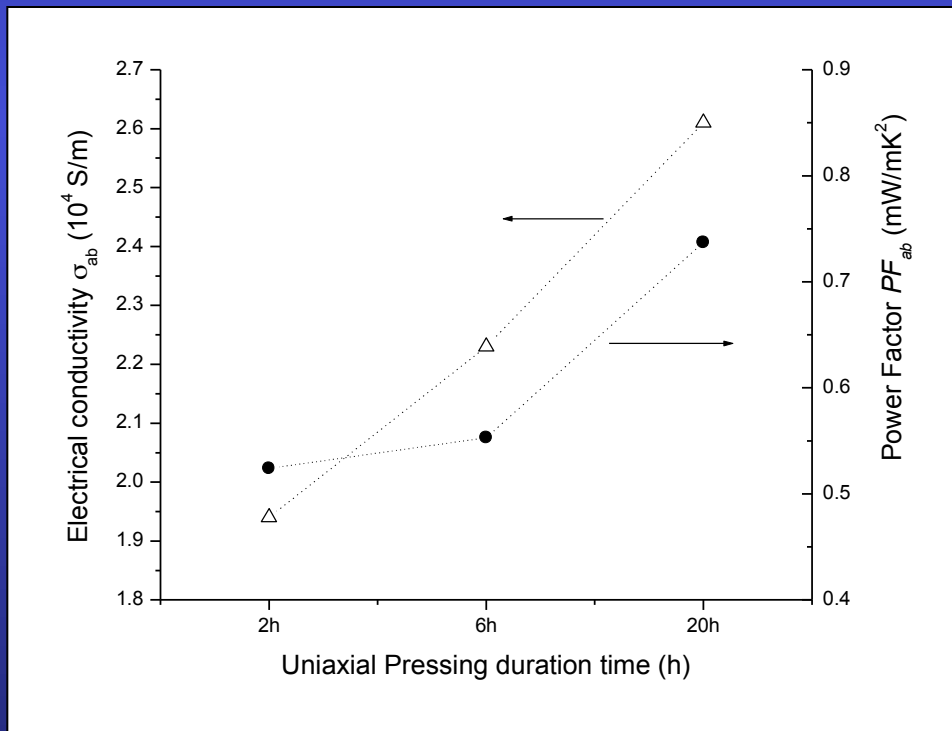
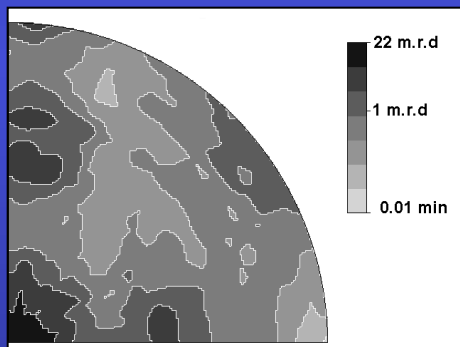
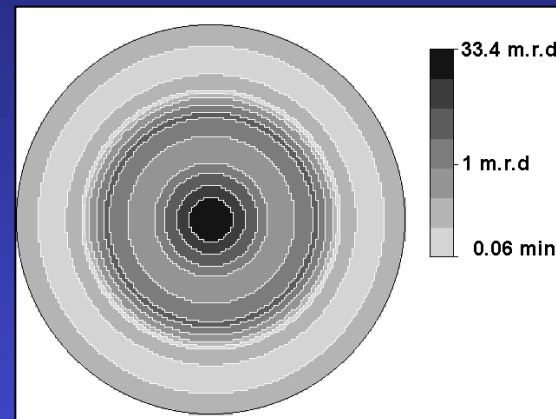
9.8 MPa for 2 h



19.6 MPa for 6 h

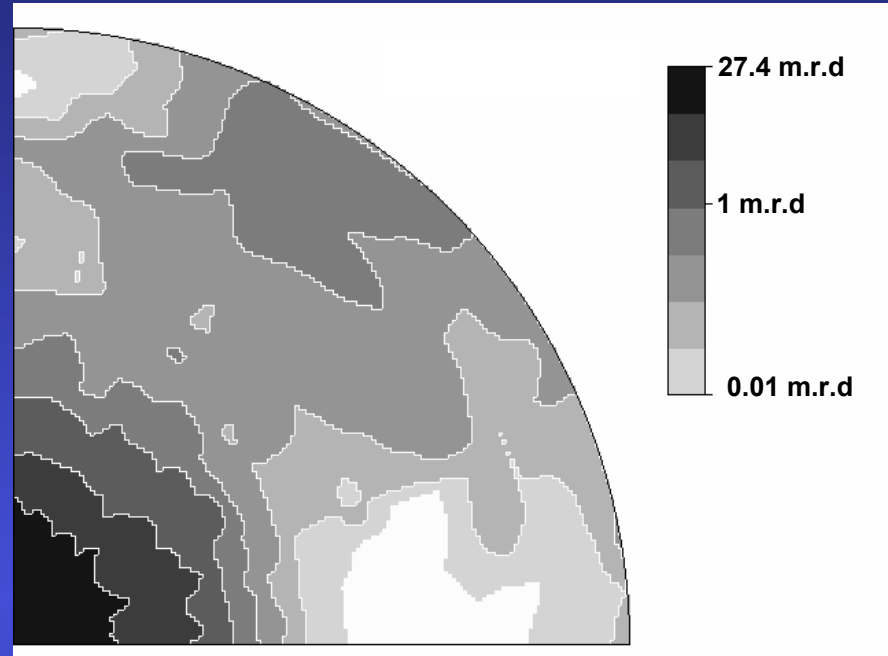


19.6 MPa for 20 h



Templated Growth Method

Logarithmic density scale, equal area projection



Magnetic Alignment



- *magnetic alignment really efficient to obtain strong textures*
- *combined analysis of modulated structures possible*

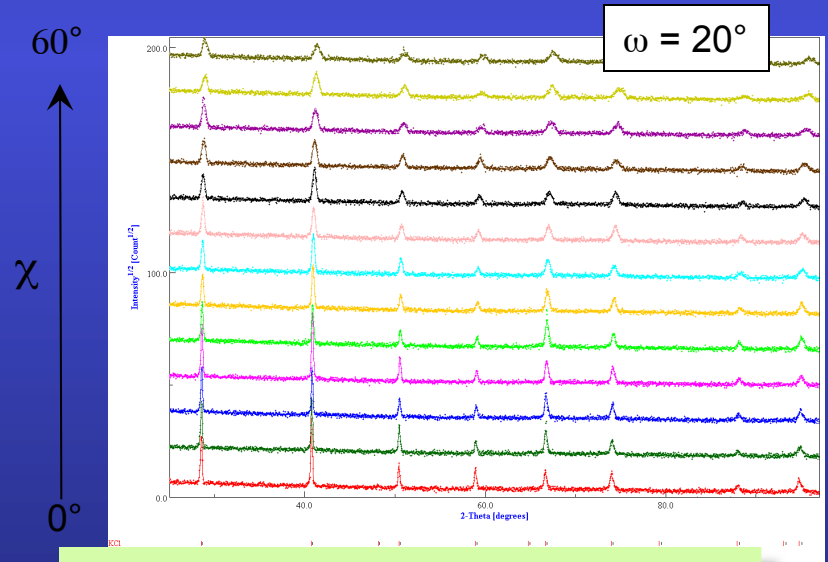
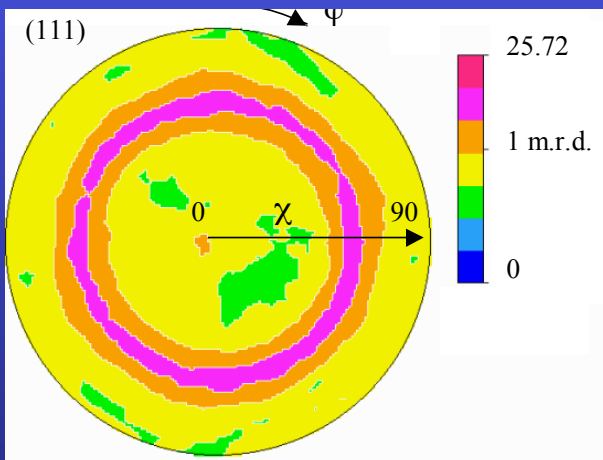
Ferroelectric PCT films

J. Ricote, DMF-Madrid

thin films:

$(\text{Ca}_{0.24}\text{Pb}_{0.76})\text{TiO}_3$ sol-gel synthesised solutions deposited by spin coating on a substrate of $\text{Pt}/\text{TiO}_2/\text{Si}$, with and without a treatment at 650°C for 30 min.

All films are crystallised at 700°C for 50 s by Rapid Thermal Processing (RTP; $30^\circ\text{C}/\text{s}$). A series is also recrystallised at 650°C for 1 to 3 h.



Refinement of individual spectra

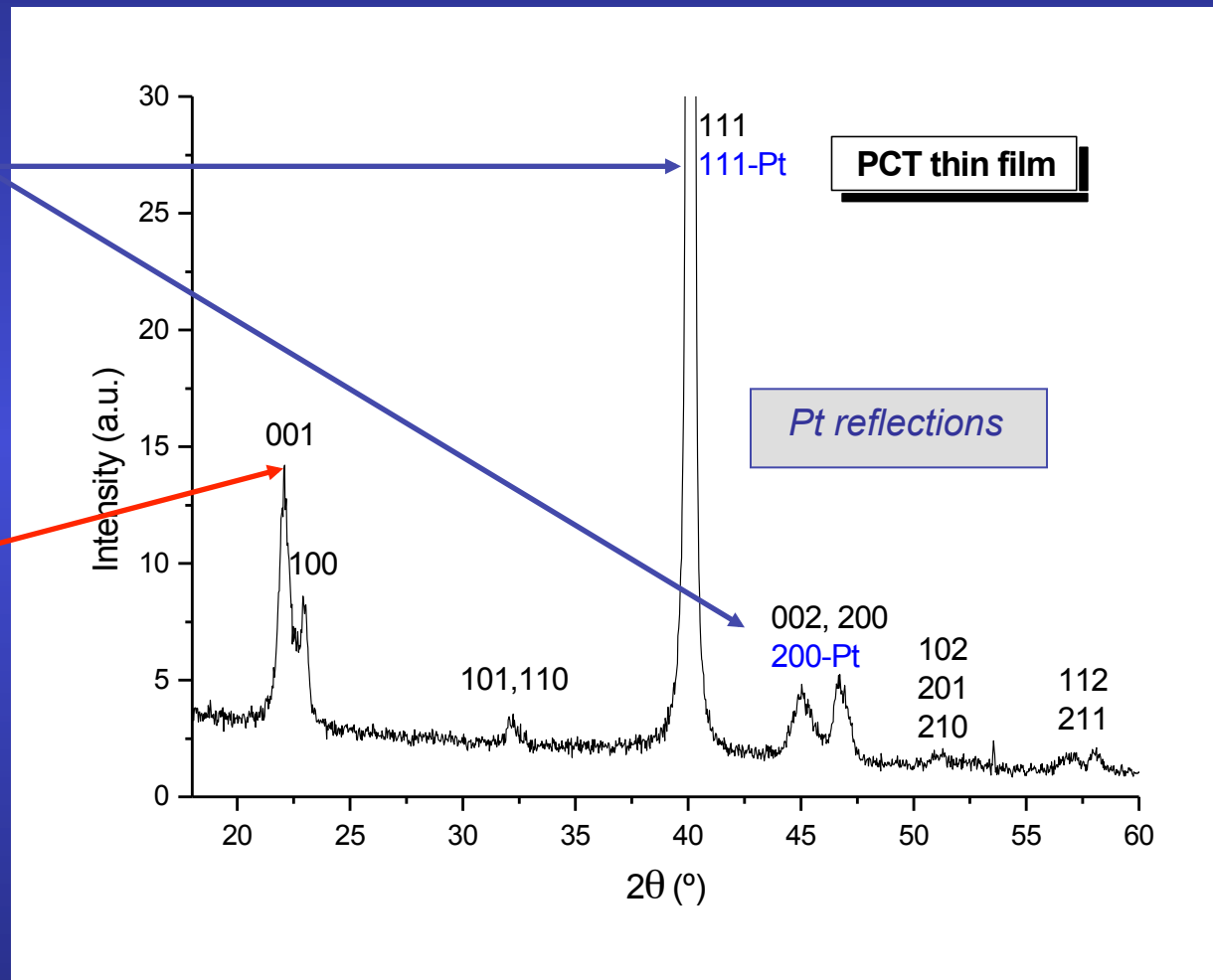
Limitations of the simple Quantitative Texture Analysis

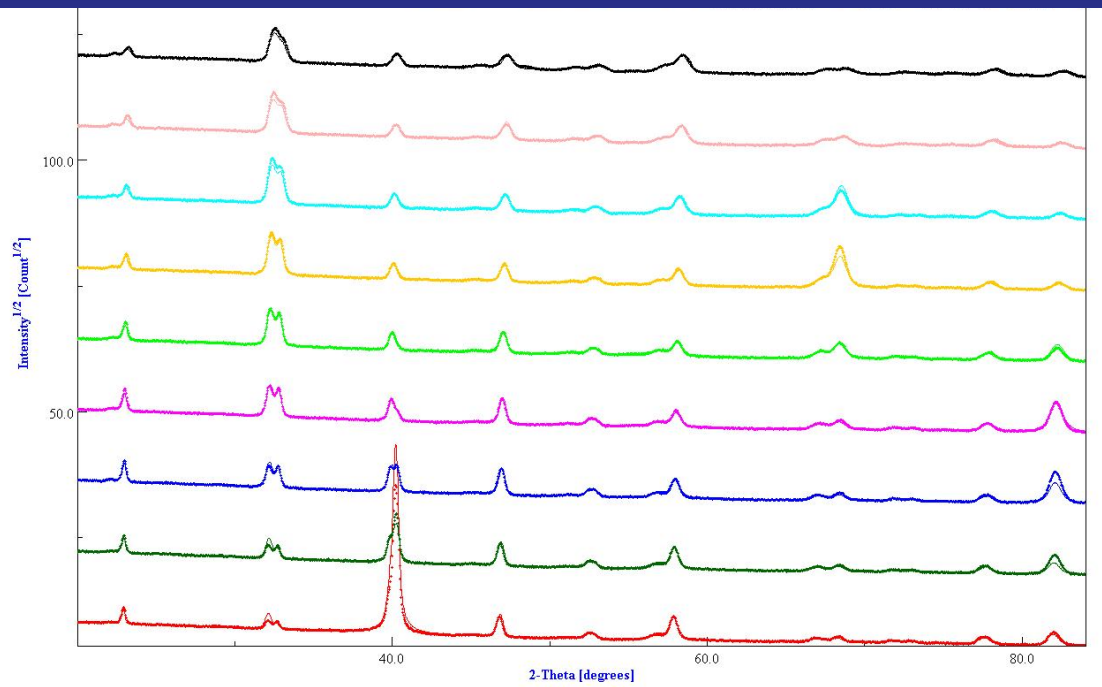
Structural parameters are difficult to obtain due to:

Substrate influence:

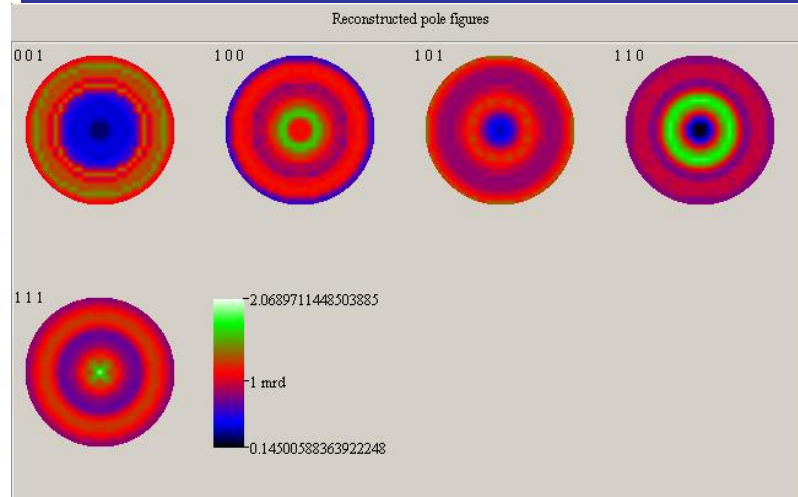
overlapping of reflections from the film and the substrate

TEXTURE effects:
peaks that do not appear at low χ angles

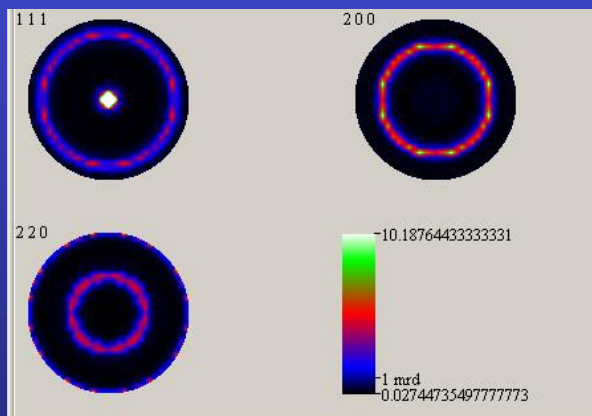




PCT



Pt

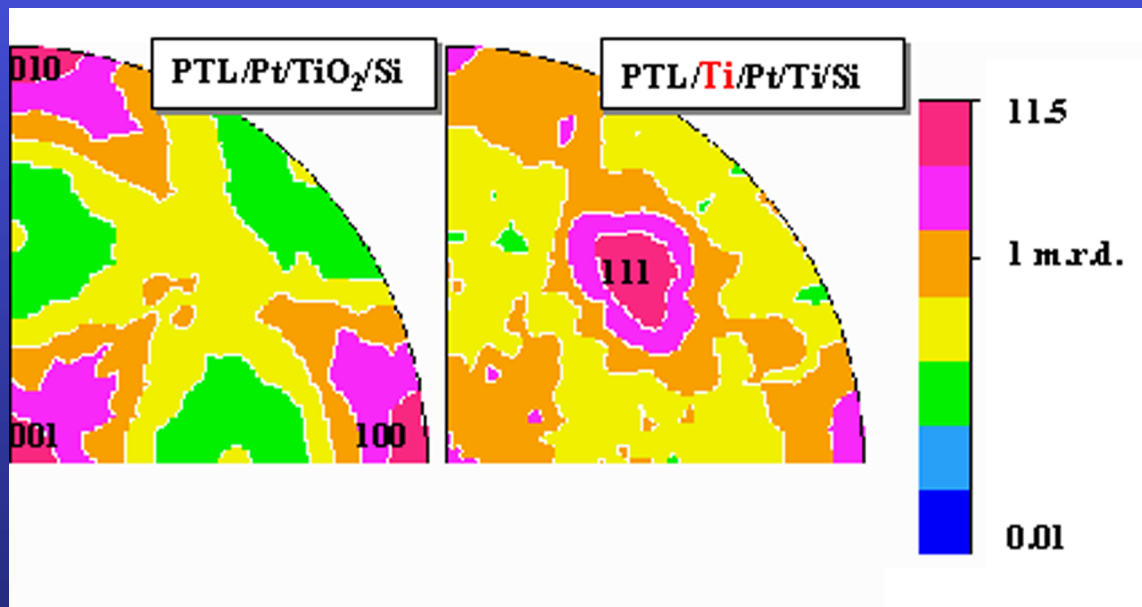


$a = 3.9108(1) \text{ \AA}$
 $T = 457(3) \text{ \AA}$
 $t_{\text{iso}} = 458(3) \text{ \AA}$
 $\epsilon' = 0.0032(1) \text{ rms}$

$a = 3.9156(1) \text{ \AA}$
 $c = 4.0497(3) \text{ \AA}$
 $T = 2525(13) \text{ \AA}$
 $t_{\text{iso}} = 390(7) \text{ \AA}$
 $\epsilon = 0.0067(1) \text{ rms}$

$R_W = 13\%$; $R_B = 12\%$; $R_{\text{exp}} = 22\%$.(Rietveld)
 $R_W = 5\%$; $R_B = 6\%$ (E-WIMV)

Atom	Occupancy	x	y	z
Pb	0.76	0.0	0.0	0.0
Ca	0.24	0.0	0.0	0.0
Ti	1.0	0.5	0.5	0.477(2)
O1	1.0	0.5	0.5	0.060(2)
O2	1.0	0.0	0.5	0.631(1)



Structural parameters

Pt layer

	a (Å)	thickness (nm)	R factors (%)
non-treated substrate			
Pt	3.9108(1)	45.7(3)	$R_W=13, R_B=12, R_{exp}=22$
annealed substrate			
Pt	3.9100(4)	46.4(3)	$R_W=8, R_B=14, R_{exp}=21$
Pt (Recryst. 1h)	3.9114(2)	47.8(3)	$R_W=9, R_B=20, R_{exp}=21$
Pt (Recryst. 2h)	3.9068(1)	46.9(3)	$R_W=9, R_B=14, R_{exp}=22$
Pt (Recryst. 3h)	3.9141(4)	47.5(9)	$R_W=27, R_B=12, R_{exp}=21$

Annealing of the substrate does not introduce significant variations on the structure of the Pt layer

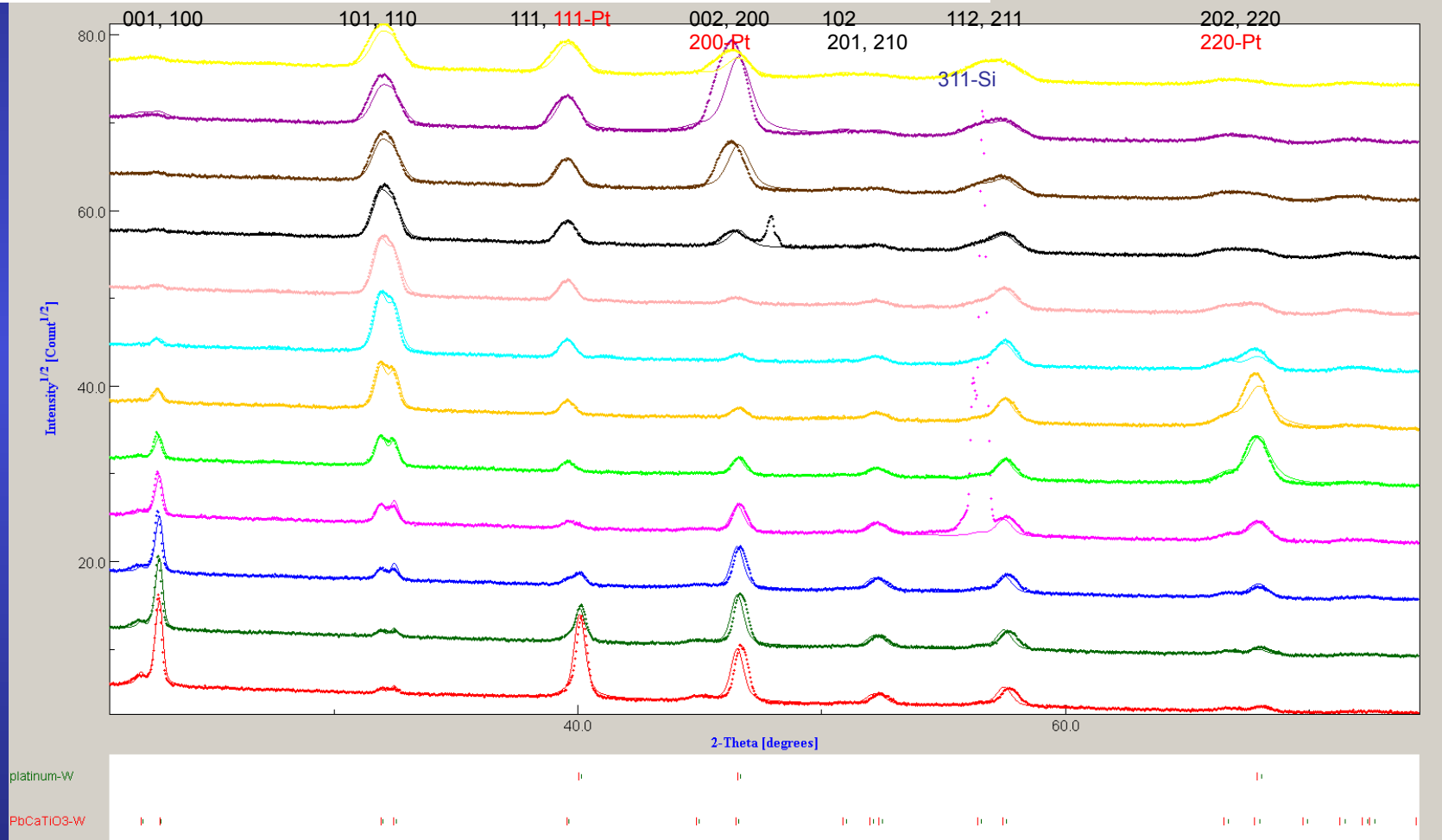
PTC film

	a (Å)	c (Å)	thickness (nm)
on non-treated substrate			
PCT	3.9156(1)	4.0497(6)	272.5(13)
on annealed substrate			
PCT	3.8920(6)	4.0187(8)	279.0(9)
PCT (Recryst. 1h)	3.8929(2)	4.0230(4)	266.1(11)
PCT (Recryst. 2h)	3.8982(2)	4.0227(4)	258.4(9)
PCT (Recryst. 3h)	3.9001(4)	4.0228(11)	253.6(29)

Recrystallisation reduces the stress on the film, and, increases the lattice parameters

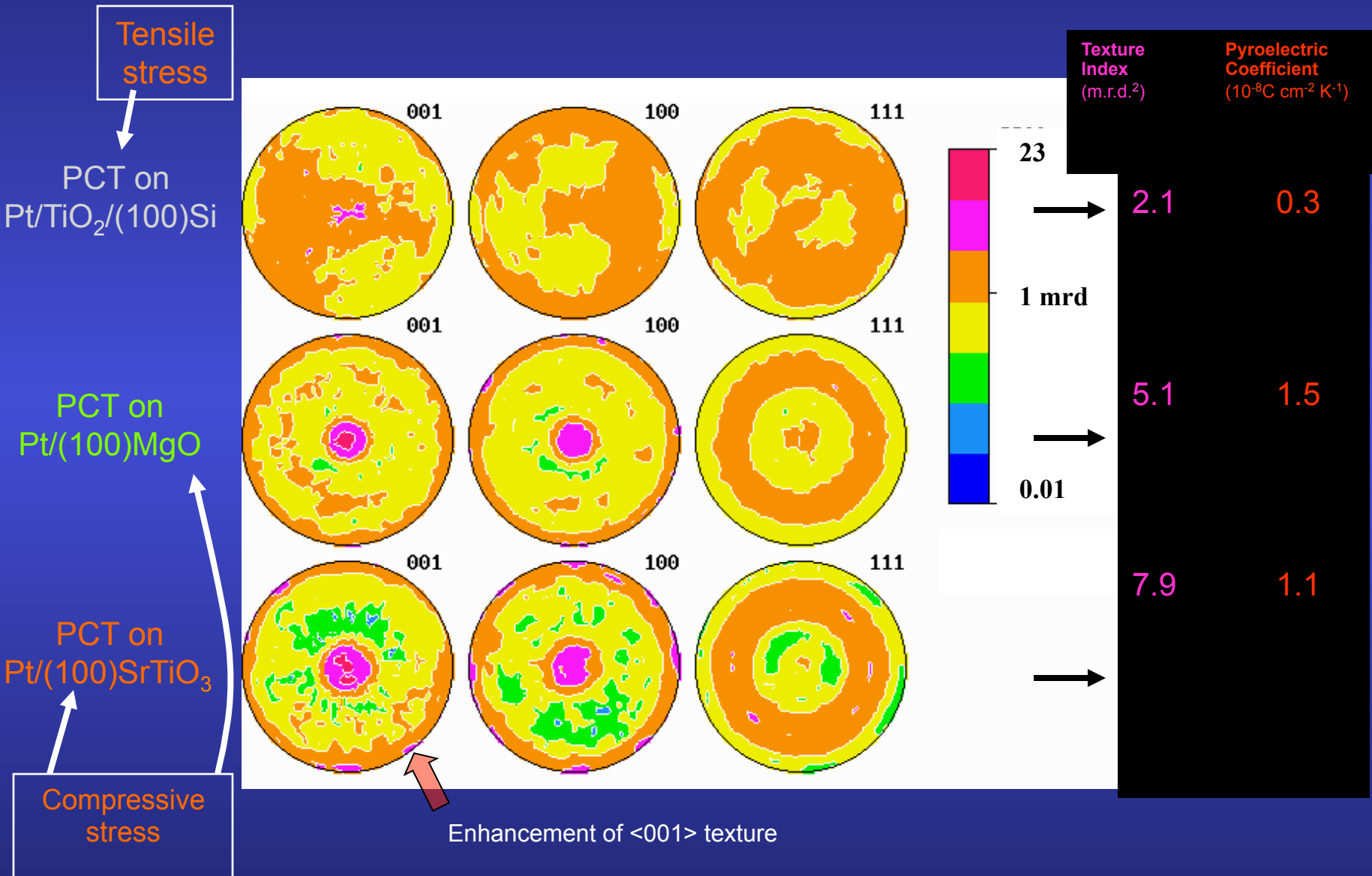
Structural, microstructural and texture quantitative characterisation of ferroelectric thin films by the combined method

Analysis of the X-ray diffraction diagrams of a PCT film on Pt/TiO₂/Si



$R_W = 13\%$; $R_B = 12\%$; $R_{exp} = 22\%$.(Rietveld)
 $R_W = 5\%$; $R_B = 6\%$ (E-WIMV)

Substrate influence on Residual Stress and Texture

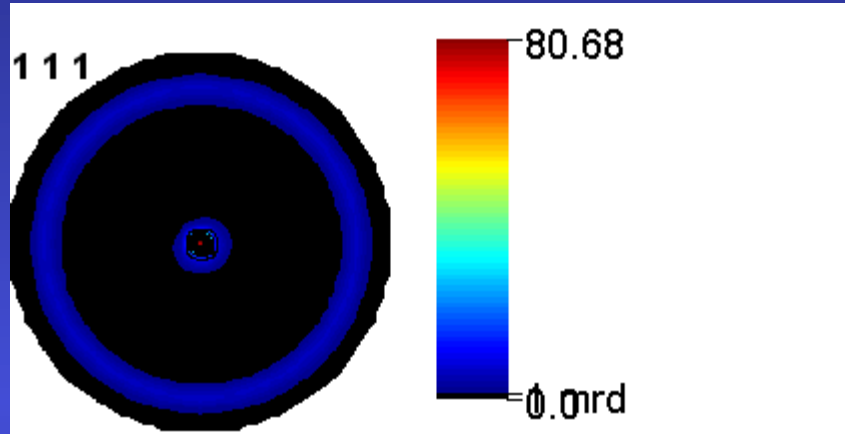


Compliance coefficients [10 ⁻³ GPa ⁻¹]	PbTiO ₃ single crystal (data set A)	Film random orientation	PCT-Si <001> contrib.≈17%	PLT <001> contrib.≈49%	PCT-Mg <001> contrib.≈68%
S ₁₁	6.5	10.1	10.5	10.0	9.7
S ₂₂	6.5	10.0	10.5	10.0	9.7
S ₃₃	33.3	9.8	9.0	10.3	11.3
S ₄₄	14.5	13.2	12.8	12.9	13.1
S ₅₅	14.5	13.2	12.8	13.0	13.1
S ₆₆	9.6	13.4	14.0	13.5	12.7
S ₁₂	-0.35	-3.3	-3.5	-3.2	-3.0
S ₂₁	-0.35	-3.3	-3.5	-3.2	-3.0
S ₁₃	-7.1	-3.2	-3.1	-3.4	-3.6
S ₃₁	-7.1	-3.2	-3.1	-3.4	-3.6
S ₂₃	-7.1	-3.2	-3.1	-3.4	-3.6
S ₃₂	-7.1	-3.2	-3.1	-3.4	-3.6
S ₃₃ /S ₁₁	5.1	0.97	0.86	1.03	1.16
S ₁₃ /S ₁₂	20.3	0.97	0.89	1.06	1.20

Geometric mean average + biaxial stress state

Ferroelectric PMN-PT films

J. Ricote, DMF-Madrid



Pt

$$a = 3.91172(1) \text{ \AA}$$

$$T = 583(5) \text{ \AA}$$

$$t_{\text{iso}} = 960(1) \text{ \AA}$$

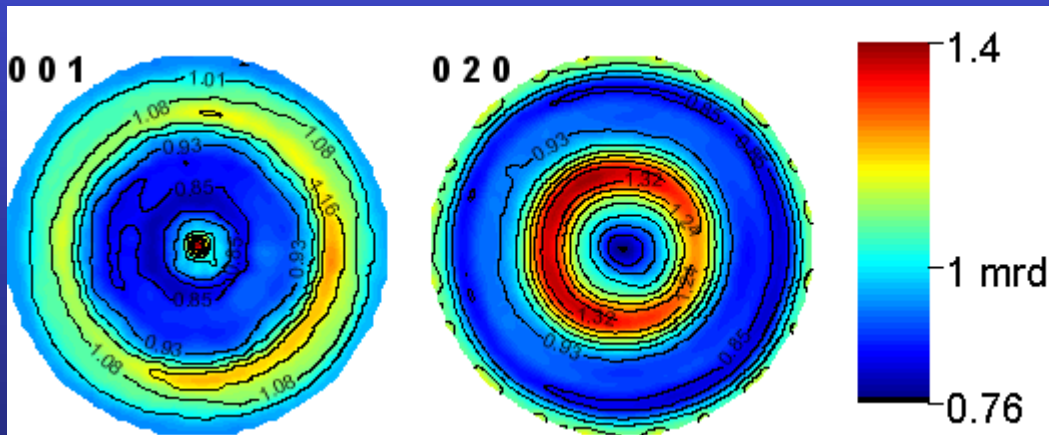
$$\varepsilon = 0.0032(1) \text{ rms}$$

$$\sigma_{11} = 0.639(1) \text{ GPa}$$

$$\sigma_{22} = 0.651(1) \text{ GPa}$$

$$\sigma_{12} = -0.009(1) \text{ GPa}$$

$\text{Pb}_{0.7}(\text{Mg}_{1/3}\text{Nb}_{2/3})\text{O}_3\text{-Pb}_{0.3}\text{TiO}_3 / \text{TiO}_2 / \text{Pt} / \text{Si-(100)}$



$$a = 5.67858(9) \text{ \AA}$$

$$b = 5.69038(9) \text{ \AA}$$

$$c = 3.99558(4) \text{ \AA}$$

$$\beta = 90.392(1) \text{ \AA}$$

$$T = 1322(9) \text{ \AA}$$

$$t_{\text{iso}} = 1338(2) \text{ \AA}$$

$$\varepsilon = 0.0067(1) \text{ rms}$$

Si nanocrystalline thin films

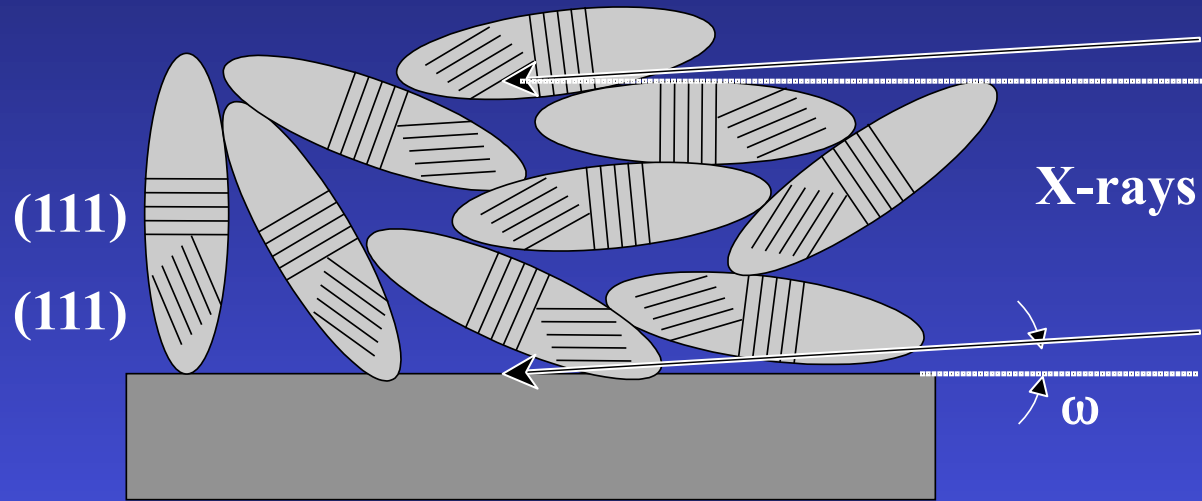
M. Morales, SIFCOM-Caen

Silicon thin films deposition by reactive magnetron sputtering:

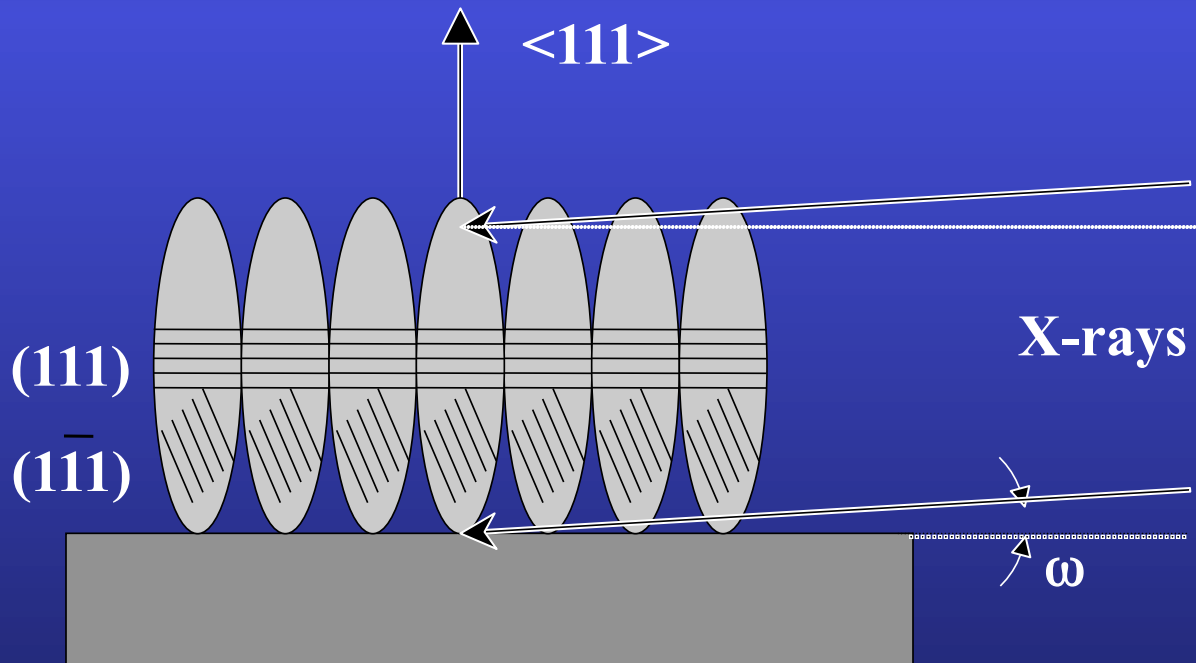
- ⇒ power density $2\text{W}/\text{cm}^2$
- ⇒ total pressure: $p_{\text{total}} = 10^{-1}$ Torr
- ⇒ plasma mixture: H_2 / Ar , $p_{\text{H}_2} / p_{\text{total}} = 80\%$
- ⇒ temperature: 200°C
- ⇒ substrates: amorphous SiO_2 (a- SiO_2)
(100)-Si single-crystals
- ⇒ target-substrate distance (d)
 - a- SiO_2 substrates: $d = 4, 6, 7, 8, 10, 12$ cm
films A, B, C, D, E, F
 - (100)-Si: $d = 6, 12$ cm
films G, H

Aim: quantum confinement, photoluminescence properties

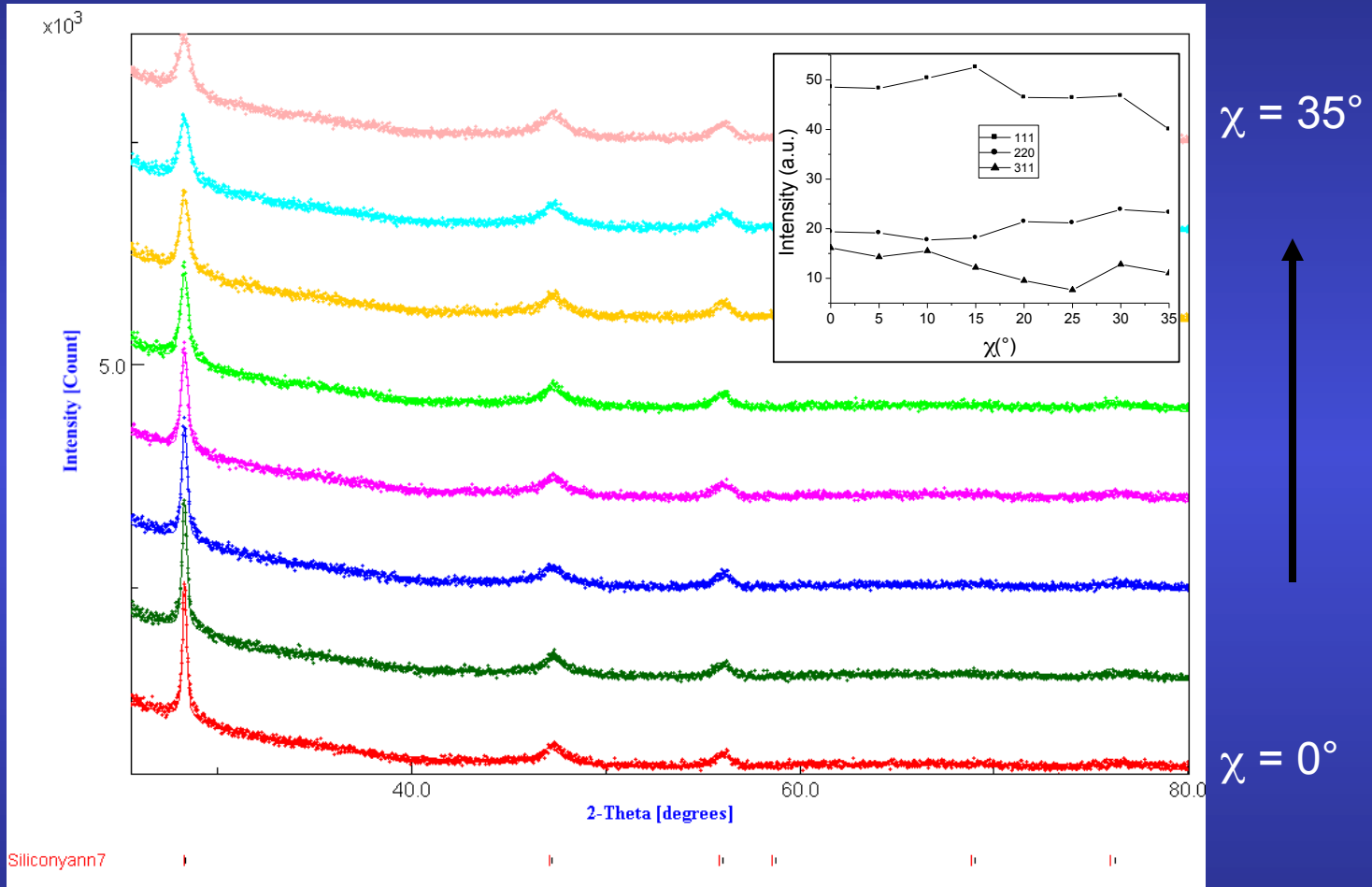
Isotropic



Textured



Typical refinement

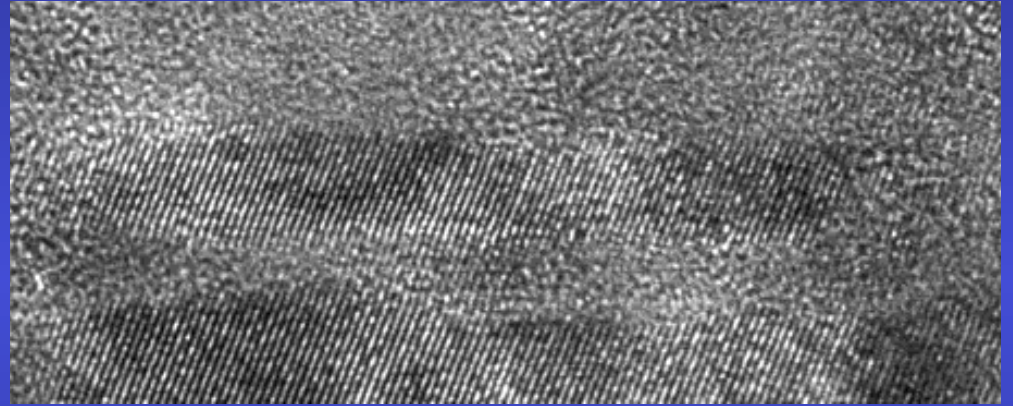
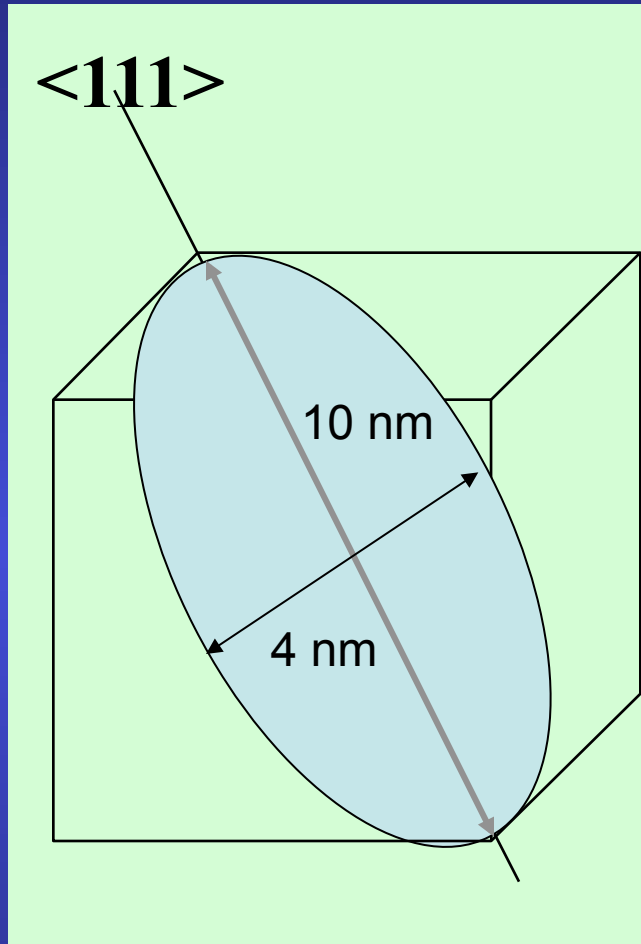


broad, anisotropic diffracted lines, textured samples

Refinement Results

Sample	d (cm)	a (Å)	RX thickness (nm)	Anisotropic sizes (Å)			Texture parameters			Reliability factors (%)			
				<111>	<220>	<311>	Maximum (m.r.d.)	minimum (m.r.d.)	Texture index F ² (m.r.d ²)	RP ₀	R _w	R _B	R _{exp}
A	4	5.4466 (3)	—	94	20	27	1.95	0.4	1.12	1.72	4.0	3.7	3.5
B	6	5.4439 (2)	711 (50)	101	20	22	1.39	0.79	1.01	0.71	4.9	4.3	4.2
C	7	5.4346 (4)	519 (60)	99	40	52	1.72	0.66	1.05	0.78	4.3	4.0	3.9
D	8	5.4461 (2)	1447 (66)	100	22	33	1.57	0.63	1.04	0.90	5.5	4.6	4.5
E	10	5.4462 (2)	1360 (80)	98	20	25	1.22	0.82	1.01	0.56	5.0	3.9	4.0
F	12	5.4452 (3)	1110 (57)	85	22	26	1.59	0.45	1.05	1.08	4.2	3.5	3.7
G	6	5.4387 (3)	1307 (50)	89	22	28	1.84	0.71	1.01	1.57	5.2	4.7	4.2
H	12	5.4434 (2)	1214 (18)	88	22	24	2.77	0.50	1.12	2.97	5.0	4.5	4.3

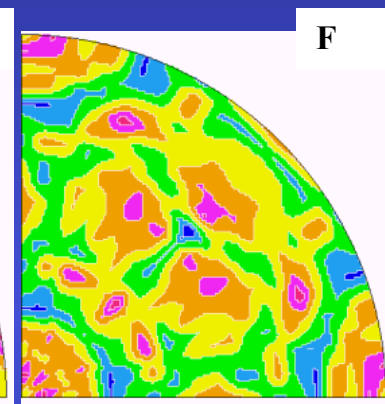
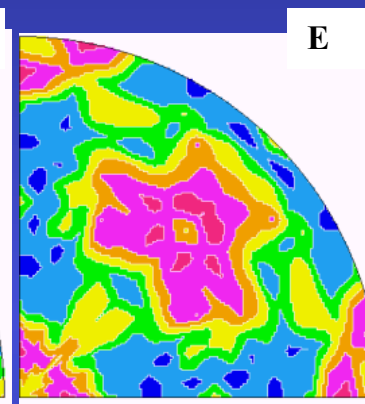
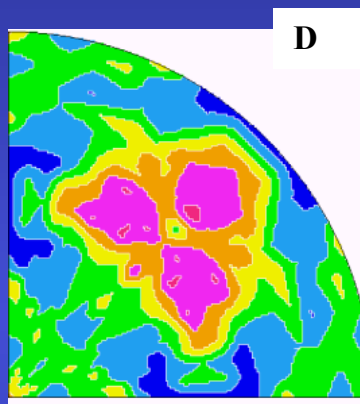
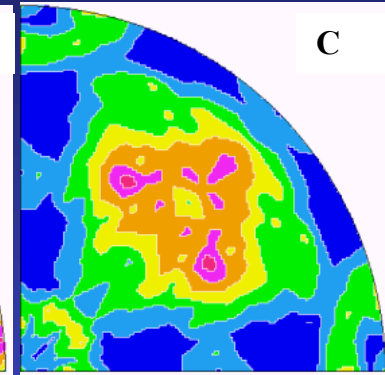
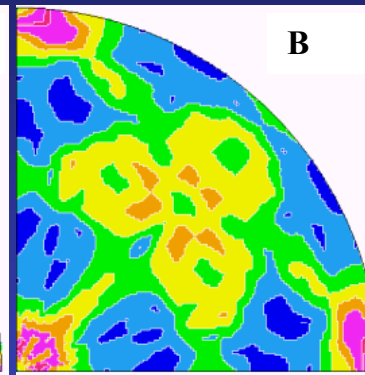
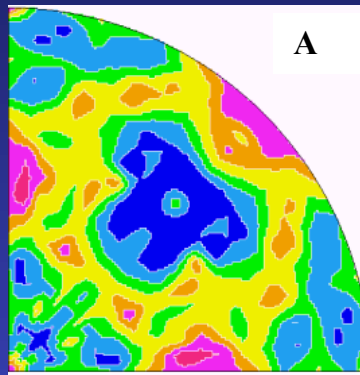
Mean anisotropic shape



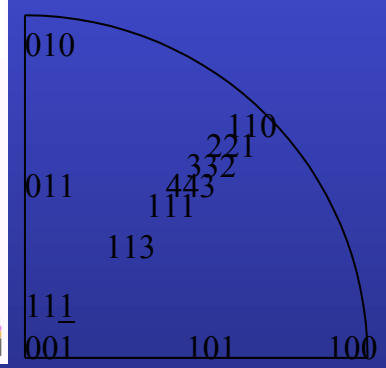
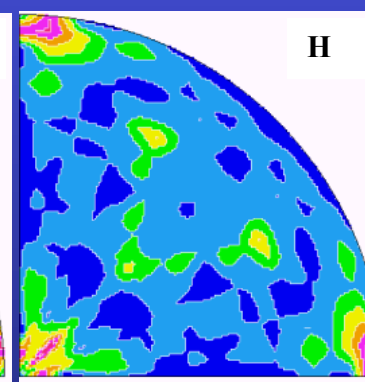
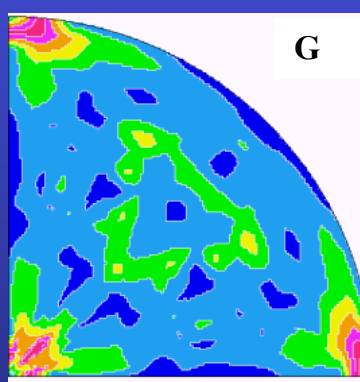
Schematic of the mean crystallite shape for Sample D represented in a cubic cell, as refined using the Popa approach and exhibiting a strong elongation along $\langle 111 \rangle$, and TEM image

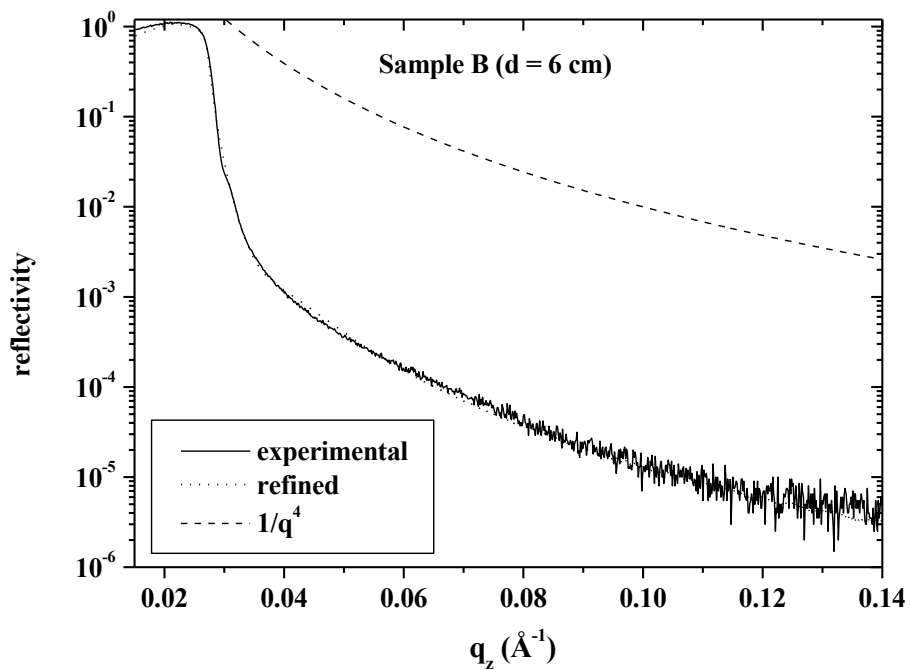
001 Inverse Pole Figures

a-SiO₂



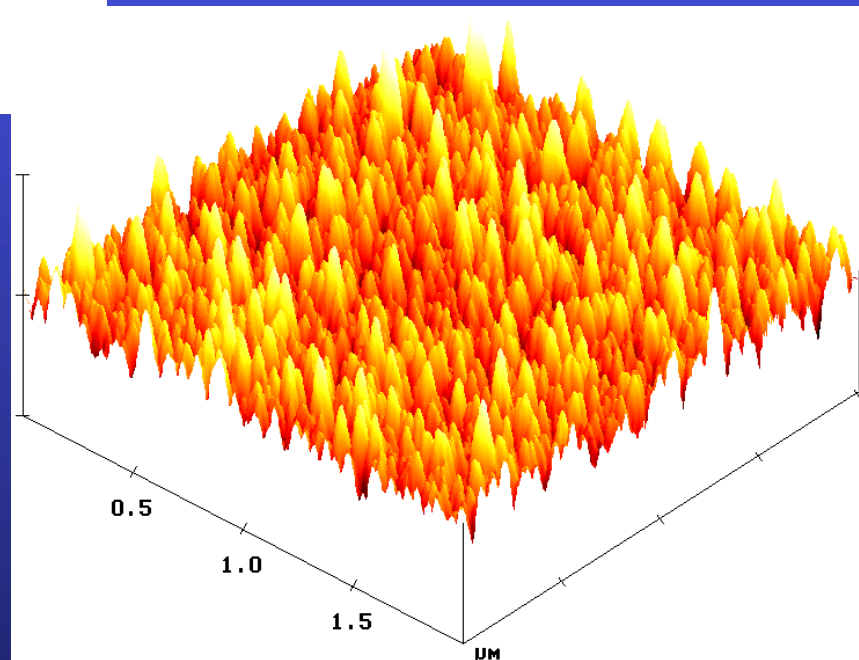
(100)-Si

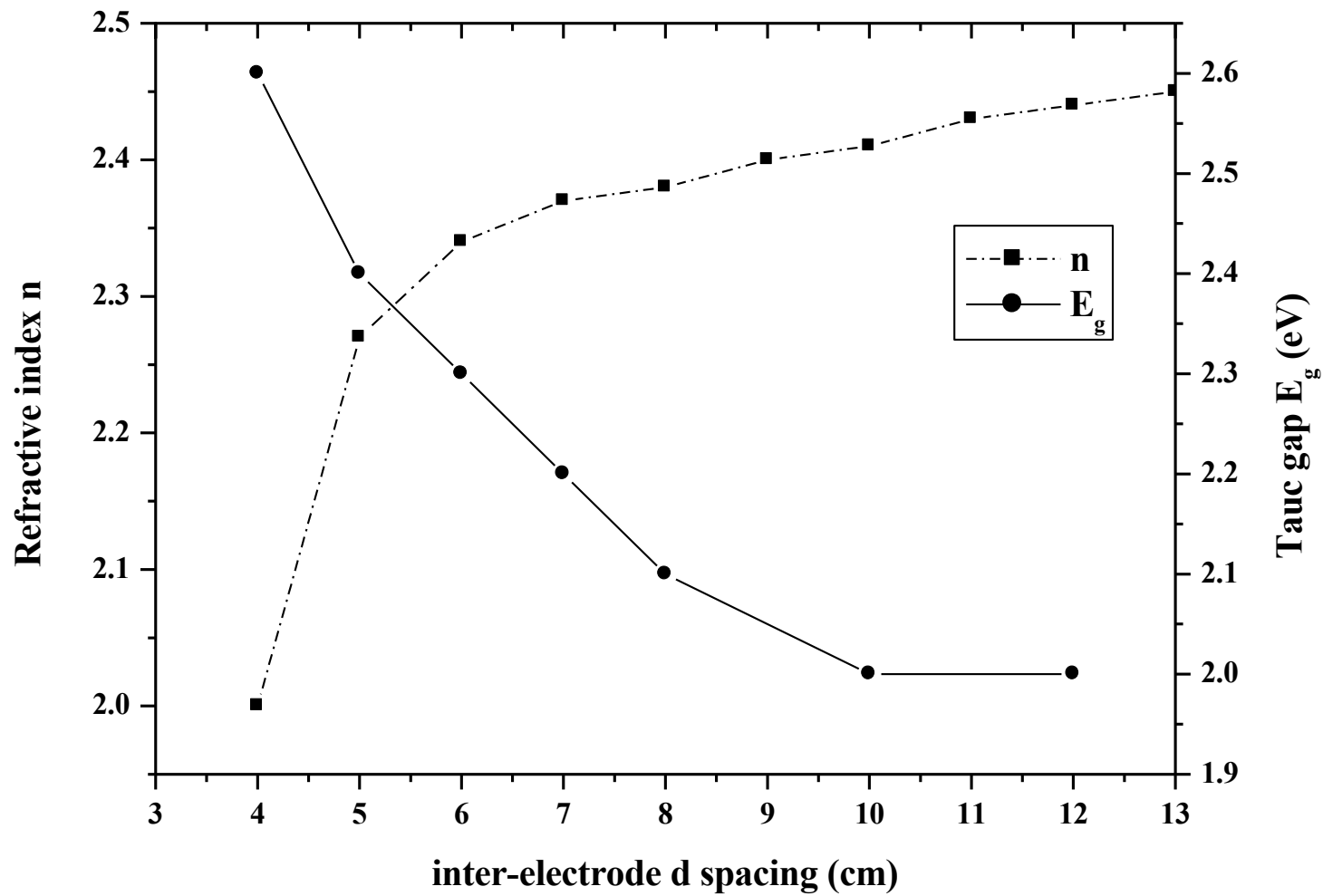




XRR:
Roughness
governed

AFM:
homogeneous
roughness

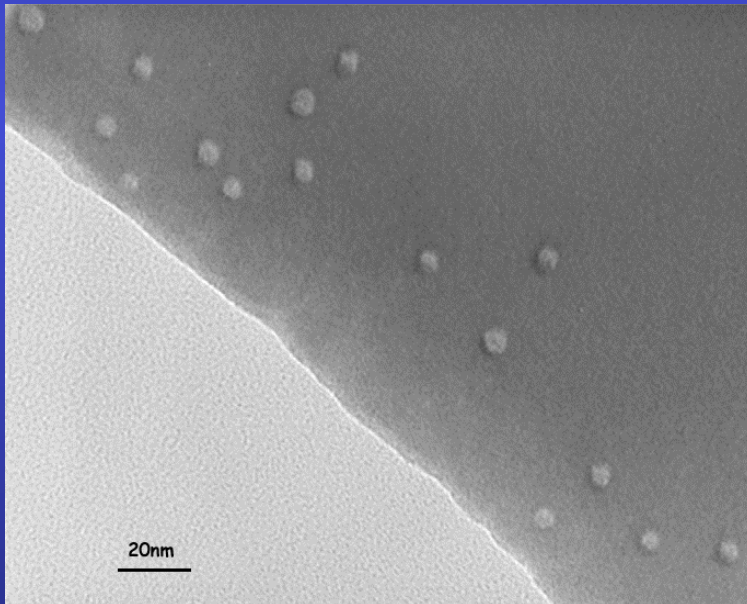




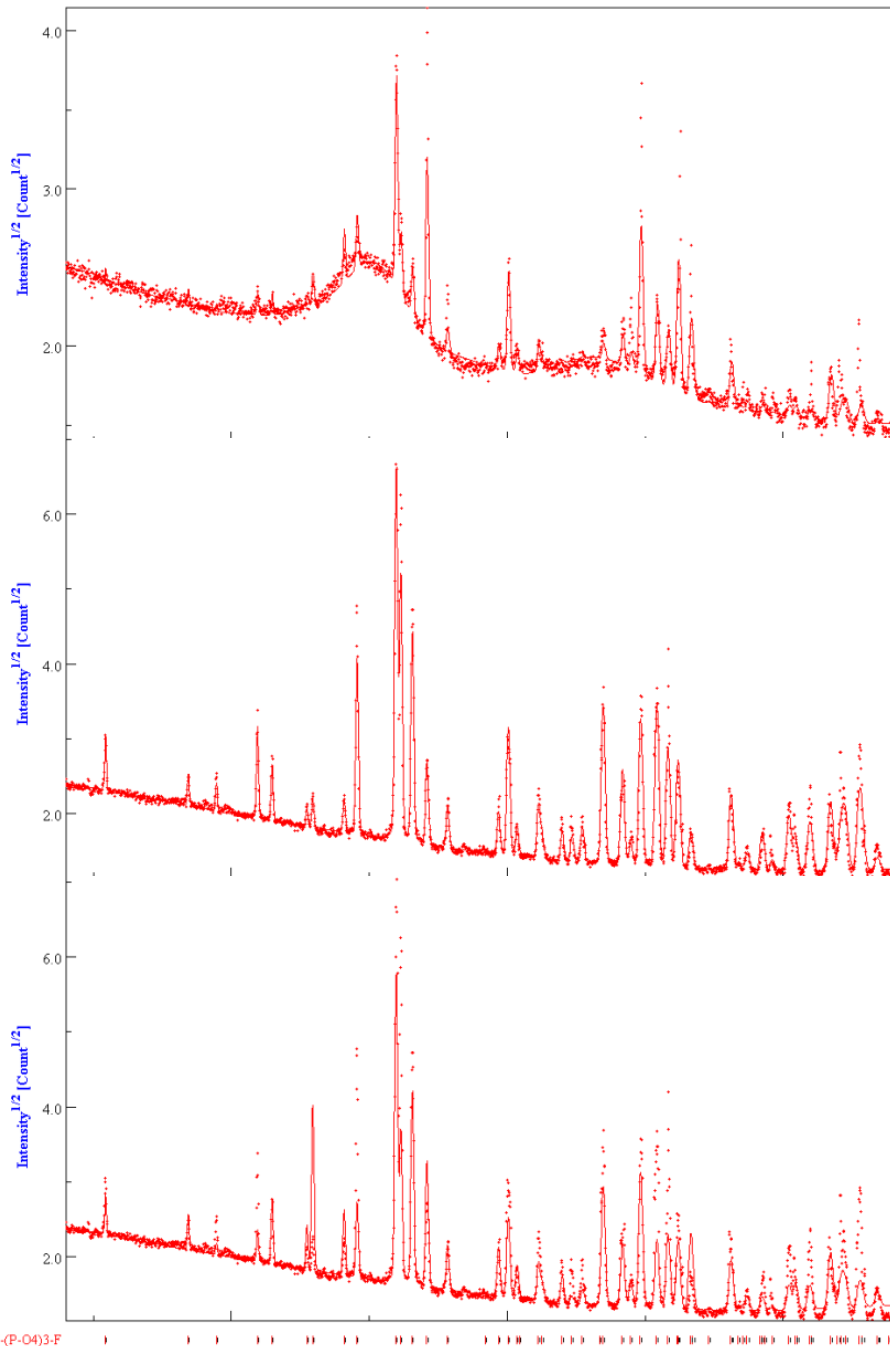
Irradiated FluorApatite (FAp) ceramics

S. Miro, PhD CRISMAT

Self-recrystallisation under irradiation, depending on $\text{SiO}_4 / \text{PO}_4$ ratio (FAp / Nd-Britholite) and on irradiating species



TEM of FAp
irradiated with 70
MeV, 10^{12} Kr cm^{-2}
ions



texture corrected,
 10^{13} Kr cm⁻²

Virgin, with texture
correction

Virgin, no texture
correction

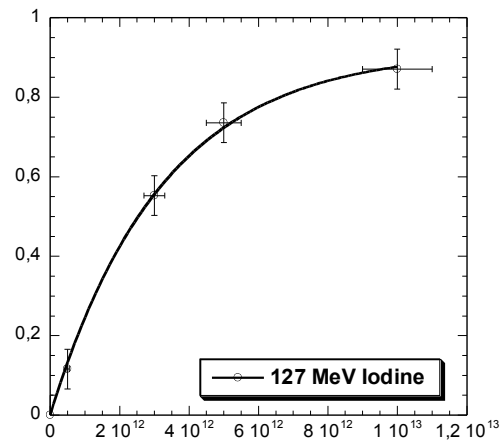
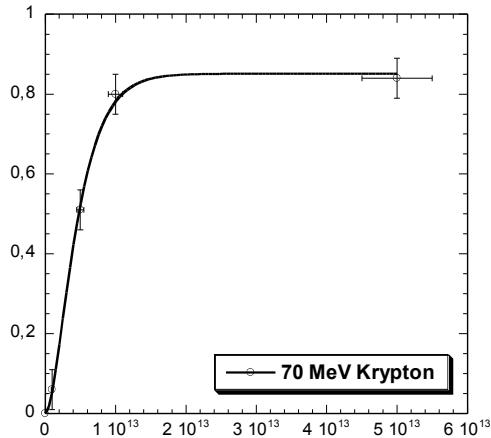
Fluence (ions.cm ⁻²)	Vc/V (%)	A (Å)	c (Å)	<t> (nm)	Δ _a /a ₀ (%)	Δ _c /c ₀ (%)	R _w (%)	R _B (%)
0	100	9.3365(3)	6,8560(5)	294(22)	-	-	14.6	9.1
Kr								
10 ¹¹	100	-	-	-	-	-		
10 ¹²	100	-	-	-	-	-		
5.10 ¹²	49(1)	9.3775(9)	6.8912(8)	294(20)	0.44	0.53	24	15
10 ¹³	20(1)	9.4236(5)	6.9105(5)	291(20)	0.94	0.82	9.9	6
5.10 ¹³	14(1)	9.3160(4)	6.8402(5)	294(22)	-0.21	-0.22	10.5	5.9
I								
10 ¹¹	-	-	-	-	-	-		
5.10 ¹¹	86(2)	9.3603(3)	6.8790(5)	90(10)	0.26	0.35	23.9	15.1
10 ¹²	-	-	-	-	-	-		
3.10 ¹²	47(2)	9.3645(3)	6.8840(5)	91(6)	0.30	0.42	13.3	9
5.10 ¹²	29.2(5)	9.3765(5)	6.8881(6)	77(11)	0.44	0.48	10.4	7.3
10 ¹³	13.2(2)	9.3719(4)	6.8857(6)	82(9)	0.38	0.45	6.7	4.9

Single impact model associated to crystal size reduction

Cell parameters and volume increase, then relax

Amorphisation / recrystallisation competition: single or double impact

Amorphous/crystalline volume fraction (damaged fraction $F_d = V_a / V$) as determined by x-ray diffraction



B

Fitting parameters	Krypton		Iodine
	Single impact $F_d = B(1 - \exp(-A\phi t))$	Double impact $F_d = B(1 - (1 + A\phi t) \exp(-A\phi t))$	Single impact $F_d = B(1 - \exp(-A\phi t))$
$A = \pi R^2$ (cm ²)	$1.85 \pm 0.15 \cdot 10^{-13}$	$4.1 \pm 0.15 \cdot 10^{-13}$	$3.3 \pm 0.15 \cdot 10^{-13}$
Radius R (nm)	2.4 ± 0.2	3.6	3.2
B (Max.damage rate)	0.87	0.85 ± 0.2	0.92 ± 0.2
χ^2	0.013	0.0006	0.0004

Conclusions

- a) Texture affects phase ratio and structure determination
- b) Microstructure (crystallite size) affects texture (go to a)
- c) Stresses shift peaks then affects structure and texture determination
- d) Combined analysis may be a solution, unless you can destroy your sample or are not interested in macroscopic anisotropy ...
- e) If you think you can destroy it, perhaps think twice
- f) more information is always needed: local probes ...
- g) www.ecole.ensicaen.fr/~chateign/texture/combined.pdf